DET NORSKE VERITAS™

Final Report

Understanding the Mechanisms of Corrosion and their Effects on Abandoned Pipelines

Petroleum Technology Alliance of Canada
Calgary, Alberta

Report No./DNV Reg No.: TAOUS813COSC (PP079627, Rev1)
March 3, 2015.

Understanding the Mechanisms of Corrosion and their Effects on Abandoned Pipelines	DET NORSKE VERITAS (U.S.A.), INC. Materials & Corrosion Technology Center 5777 Frantz Road Dublin, OH 43017-1886, United States Tel: (614) 761-1214 Fax: (614) 761-1633 http://www.dnv.com http://www.dnvusa.com
For: Dr. Soheil Asgarpour Petroleum Technology Alliance of Canada Suite 400, 500 Fifth Avenue S.W. Calgary, Alberta	
Account Ref.:	

Date of First Issue:	March 3, 2015	Project No.	PP079627
Report No.:		Organization Unit:	Materials & Corrosion Technology Ctr.
Revision No.:	1	Subject Group:	
Summary:			
Please see Executive Summary.			
Prepared by:	Colin Scott PhD, PEng Senior Engineer	*Signature*	
Verified by:	John A. Beavers, PhD, FNACE Director – Forensic Investigation	*Signature*	
Approved by:	Oliver C. Moghissi, PhD Vice President, Pipeline Services	*Signature*	

☑	No distribution without permission from the client or responsible organizational unit (however, free distribution for internal use within DNV after 3 years)		
☐	No distribution without permission from the client or responsible organizational unit	Key Words	
☐	Strictly confidential		
☐	Unrestricted distribution		

Rev. No. / Date:	Reason for Issue:	Prepared by:	Approved by:	Verified by
Rev0; 2/7/2014	Original issue	CS	OCM	JAB
Rev1; 3/3/2015	Incorporation of review comments	JAK	JAB	CJM

Executive Summary

Pipeline abandonment occurs when a pipeline is permanently removed from service at the end of its useful life. Pipelines removed from service may be either abandoned in place, or they may be excavated and physically removed. The potential impacts of either approach require consideration.

Abandoned pipelines may not have operational cathodic protection systems. This allows the pipe material to corrode with time, and the pipeline loses structural integrity. The pipe wall of an abandoned pipeline is not needed to contain product, as it is in service, but it is necessary to support the weight of the soil overburden and any traffic over the pipe. A pipeline that degrades sufficiently due to natural corrosion processes could, in principle, collapse under the weight of soil above the pipe and any traffic, if present. The traffic may be vehicular if the pipeline crosses under roads, rail lines, or it may be agricultural equipment if the pipeline crosses farmland.

The objectives of this project were to develop corrosion rate, structural integrity and soil collapse models to better understand the susceptibility of buried onshore pipelines to collapse following abandonment and long-term corrosion degradation.

In general terms, predictions indicate pipelines maintain sufficient structural integrity to resist collapse due to personal or vehicular traffic for a large number of years. The word “large” is relative and will change based on specific circumstances, but, for most cases, is in the order of hundreds to thousands of years.

To support these predictions, a literature review was performed to identify corrosion and structural integrity studies relevant to the development of predictive models to understand the degradation and collapse of abandoned pipelines. Several industry studies have been performed by other researchers that are directly relevant to this program. The data generated and the models developed by these studies were reviewed.

Soils data generated by the National Bureau of Standards (NBS) were used to develop a corrosion rate model that is considered suitable for the pipeline abandonment program. The model is based on a parabolic rate law, and provides a reasonable upper bound estimate for corrosion rate calculations. The model can be modified easily to account for average or lower bound corrosion rate conditions. The methodology of the model was discussed. Examples and plots are provided to demonstrate the use and sensitivity of the model.

Established structural integrity and soil mechanics equations, developed primarily by the civil engineering industry and academia, were combined to develop a structural model considered suitable for the pipeline abandonment program. The model is based on the assumption that soils loads and live loads acting above the pipe will lead to either plastic or elastic collapse of the

pipeline at a critical load. The critical load acting on the pipe to cause this collapse is considered the load bearing capacity of the pipeline. The model can be modified to account for dry or wet soils, jacked installation of the pipeline, and personnel or vehicle traffic. The methodology of the model were discussed. Simple examples and plots are provided to demonstrate the use and sensitivity of the model.

As shown by the analytical results of this study, the predicted time to collapse will vary depending on a number of variables, including (i) pipeline diameter, wall thickness and yield strength, (ii) soil type and soil properties, and (iii) pipeline depth of cover. Accordingly, analytical predictions have to be made on a case-specific basis using applicable pipeline and soil data.

The analysis suggests that a medium diameter pipeline situated in stable soil and at typical depth would support a personal truck for approximately 9,000 years before collapse. On the other hand, in a situation where a large diameter pipeline is buried at very shallow depth in extremely poor soil conditions, the pipeline may collapse under the weight of a truck in the time of approximately 100 years.

Note that the above examples assume the pipelines are not coated and the bare steel surface is free to corrode. Generally, this is an inherently conservative assumption because there is no coating to retard the degradation of the pipe steel. If a coating were present, as is typically the case, the model would predict a higher load bearing capacity and / or a longer time to collapse. In some cases, corrosion rates can be faster at areas of coating disbondment than for a bare pipeline.

The corrosion rate and structural integrity models can be combined in a practical way to determine the load bearing capacity of the pipeline as a function of time. Instructions and examples are provided in the use of the models. In addition, both bare steel pipelines and pipelines with coating and partial disbondment were considered and discussed.

A geometric model was developed to estimate the depth of soil subsidence in the event that a pipeline does collapse. The predicted depth of subsidence is highly variable depending on pipeline diameter, burial depth and soil type, but is generally expected to be less than 10 cm. At the very extreme, the predicted depth of subsidence could be up to about 40 cm for a large diameter pipeline buried at shallow depth in poor soil conditions. The area of disturbance would be much wider than the pipeline diameter due to the behavior of soil above the pipe.

The models developed within this study need further development and refinement.

Table of Contents

List of Tables

List of Figures

List of Symbols

A	area (m^2)
B'	coefficient of support
C	depth of soil cover (m)
d	depth of corrosion (mm)
D	outside diameter of pipe (m)
E	modulus of elasticity (GPa)
E'	soil modulus (MPa)
F'	impact factor for live loads
FS	factor of safety
h	horizontal offset distance between applied point load and pipe centre line (m)
I	second moment of area (m^4/m)
k_{ml}	curve fit coefficient (mass loss)
k_p	curve fit coefficient (penetration)
K	bedding factor
L	lag factor
n	curve fit exponent
P_{cap}	critical load bearing capacity *defined as a force* (N)
P_{live}	live load acting at surface level, *defined as a force* (N)
P_{pipe}	load on pipe at depth due to live load acting at surface level, *defined as a pressure* (MPa)
P_{soil}	load on pipe at depth due to weight of soil, *defined as a pressure* (MPa)
R	radius of pipe (m)
R_w	buoyancy factor
S	depth of subsidence due to pipeline collapse (m)
t	wall thickness of pipe (mm)
t_o	initial or nominal wall thickness of pipe (mm)
T	time (years)
T_p	time of penetration (years)
Δy	vertical deflection of pipe (m)
γ	dry unit weight of soil (N/m^3)
σ_{bend}	bending stress (Pa)
σ_{flow}	the average of yield strength and ultimate tensile strength (σ_{yield+} σ_{yield})/2 (Pa)
σ_{yield}	yield strength of pipe steel (Pa)
λ	soil cohesion (kPa)

1.0 BACKGROUND

Pipeline abandonment occurs when a pipeline is permanently removed from service at the end of its useful life. Pipelines removed from service may be either abandoned in place, or they may be excavated and physically removed. The potential impacts of either approach require consideration.

Abandoned pipelines may not have operational cathodic protection systems. This allows the pipe material to corrode with time, and the pipeline loses structural integrity. The pipe wall of an abandoned pipeline is not needed to contain product, as it is in service, but it is necessary to support the weight of the soil overburden and any traffic over the pipe. A pipeline that degrades sufficiently due to natural corrosion processes could, in principle, collapse under the weight of soil above the pipe and any traffic, if present. The traffic may be vehicular if the pipeline crosses under roads, rail lines, or it may be agricultural equipment if the pipeline crosses farmland.

Various regulatory and industry bodies have collaborated to discuss technical and environment issues related to pipeline abandonment. In 1996, representatives from the Canadian Association of Petroleum Producers (CAPP), the Canadian Pipeline Association (CEPA), the Alberta Energy and Utilities Board (AEUB) and the National Energy Board (NEB) prepared a Discussion Paper[1] outlining technical and environmental considerations relevant to pipeline abandonment. The paper considered ground subsidence, and discussed the effects of corrosion of pipe material and soil mechanics on the likelihood and consequences of soil collapse. Data provided indicated corrosion on less than 1% of the pipeline surface area, due to the presence of a generally intact corrosion protection coating. However, the report did not discuss coating degradation over time. The conclusion was that pipelines would take several decades or more to lose substantial structural integrity. The supporting modelling concluded that collapse of pipelines of 323.9 mm (nominal 12 inch) diameter or less would lead to negligible subsidence.

A 2007 report [2] by the Terminal Negative Salvage Working Group and Steering Committee of CEPA reiterated the issues of concern raised by the 1996 NEB study. In late 2007, the NEB established the Land Matters Consultation Initiative (LMCI) to consider land related matters with input from various stakeholders. The LMCI worked with various industry members and land ownership groups to increase understanding between parties and identify areas of improvement. An outcome of their work was a “roadmap for change” to achieve a balance amongst stakeholders’ concerns. In 2010, the NEB commissioned a literature review to summarize known technical issues related to pipeline abandonment and to identify knowledge gaps for future study [5]. The review recommended several future studies, including work on corrosion rate modelling and degradation of pipelines, structural modelling of pipelines and soil collapse modelling.

The Petroleum Technology Alliance of Canada (PTAC) was established in 1996, as a not-for-profit association to support Canada's hydrocarbon energy industry leadership through innovation and technology development. PTAC and CEPA established the Pipeline Abandonment Research Steering Committee (PARSC) to guide research to address knowledge gaps identified by the NEB 2010 study. In March of 2013, the PARSC issued a request for proposals to commission research projects on three topics. One of the topics; PARSC 001 "Understanding the Mechanisms of Corrosion and their Effects on Abandoned Pipelines" is the subject of this report.

The PARSC 001 Project Description identified three sub-projects:

1. Validation of Corrosion Models for Abandoned Pipelines.
2. Structural Integrity Study.
3. Collapse of soil under different void sizes, soil types, and depth of pipeline cover – definition of research scope.

The three sub-projects are inter-related, and it was proposed by DNV that all three sub-projects would be performed concurrently. The advantage of this is that all three sub-projects are developed with a common philosophy, and can be used together.

The first of the sub-project relates to corrosion models, with the goal to develop an estimate of the degradation of the pipe material as a function of time. The second sub-project relates to loss of structural integrity as the pipe degrades. By combining the two sub-projects, it becomes possible to develop a model in which the structural integrity of the pipe can be estimated as a function of time. If the pipe structural integrity degrades sufficiently, the pipe may collapse under the weight of soil above the pipe and vehicle traffic, if present. By studying soil collapse as part of the third sub-project, it then becomes possible to estimate the susceptibility to soil collapse as a function of time. It was also considered by DNV that the structural integrity of the pipe and the soil void would be contingent on one another and these two sub-projects should be developed together. Although the three sub-projects required different expertise (ie. corrosion, structural integrity, soil mechanics), the development of a single, unifying model is considered by DNV to be of overall benefit.

2.0 METHODOLOGY

The three sub-projects were developed as follows:

2.1 Sub-Project 1 – Validation of Corrosion Models for Abandoned Pipelines

The first stage of Sub-Project 1 was to perform a literature review of relevant corrosion models. The information, and particularly the lessons learned during the development of the models, was compiled as a starting point for the continued model development. Both external and internal corrosion were considered.

The California State Department of Transportation [11] analyzed data from perforated culverts and developed a model to estimate the time to perforation as a function of soil pH and resistivity. This model could be adapted to thicker wall pipelines that are of particular interest to the program. The model was reviewed and modifications were considered to improve its applicability to thicker wall pipe.

Another approach was to consider the generic corrosion rates of steels in various soils. The National Bureau of Standards performed extensive research in the 1950's and a summary of the work is available [17]. This work was reviewed and considered with respect to modelling of corrosion rates in abandoned pipelines. Analysis of the data allowed corrosion rates to be estimated as a function of soil properties. Soil types were grouped by corrosivity and a generic rate determined for each group. Models were developed that consider both general wall loss and pitting.

It is also of interest to consider internal corrosion. Moisture accumulation at the bottom of pipes is a known corrosion issue for pipes in service. However, loss of metal at the bottom of the pipeline will not necessarily lead to loss of structural integrity, and this was considered during the structural integrity study.

Models, whether developed or modified, will need to be validated using data from pipelines that have previously been abandoned. This requires both review of available documentation, and a continued effort to collect information as abandoned pipelines are inspected in the future.

An issue of tacit interest to the program is coating degradation. The majority of underground pipelines are protected from corrosion by both a corrosion resistant coating and a cathodic protection system. Abandonment of a pipeline may lead to a loss of cathodic protection, but will not lead to an immediate loss of coating integrity. Corrosion rates at areas of disbonded coating were determined during the development of the models. However, the proportion of a pipeline that is un-coated is low, likely less than one percent. Corrosion at areas of disbonded coating may lead to the coalescence of adjacent corrosion anomalies and/or perforation. Consequently, the structural integrity of the pipe would be degraded and the eventual structural collapse of the pipe and soil is possible.

2.2 Sub-Project 2 – Structural Integrity Study

The first stage of Sub-Project 2 was to perform a literature review of similar industry studies on structural integrity. The models developed for these standards were reviewed and their applicability considered. Both general wall loss and pitting were considered. Given that most pipelines are coated, it is unlikely that general wall loss is the primary issue of interest. The structural integrity of pipelines containing multiple small perforations is considered more realistic.

Fitness for service assessments, such as those described by API579-1/ASME FFS-1 [45], are typically focused on pipelines subject to internal service pressure. However, they do consider pipelines subject to external pressures, and in some cases, consider elastic collapse under hydrostatic pressures. In the case of abandoned pipelines under soil loading, the loads are not hydrostatic, and this must be considered in the assessment. Loads from soil weight and vehicle traffic lead to a downwards force on the pipe. The soil at the sides of the pipe acts to constrain the pipe and prevent collapse. The stress acting on the top of the pipe and in the wall of the pipe can be estimated using established models. Soil mechanical properties become important to the assessment.

Existing models were considered and modified as appropriate to address the issue of pipeline collapse. The models developed were combined with the results of the corrosion modelling work to develop a model that estimates the time to collapse of a given pipeline, as a function of soil properties, and pipeline dimensions, depth of cover and surface loads.

2.3 Sub-Project 3 – Collapse of Soil under Different Void Sizes, Soil Types and Depth of Pipeline Cover – Definition of Research Scope

In the event that there is sufficient load acting on a pipe to cause collapse, the soil would collapse into the void of the empty pipe. It is of interest to the study to estimate how deep the soil would collapse. A simple geometric model was developed to determine the depth as a function of pipe diameter and depth of cover.

The goal of Sub-Project 3 was to define and propose research scopes to validate the structural integrity and soil collapse models. Three methodologies were proposed (by PTAC) to study soil collapse. These methods were to examine previously abandoned pipelines, bury and remove lengths of pipe to monitor soil collapse, and build physical soil models with voids and test in centrifuges. Additional methodologies were proposed by DNV. These were to test soil void collapse in a laboratory, and to model soil void collapse using finite element analysis. These methodologies are not discussed further in this report.

3.0 LITERATURE REVIEW

3.1 Corrosion Rates of Steels in Soil

3.1.1 The Fundamentals of Corrosion

Corrosion is the degradation of a metal due to natural electrochemical reactions. Electrochemical reactions consist of two "half-cell" reactions; the anodic reaction and the cathodic reaction. The anodic reaction involves a loss of electrons, and is referred to as "oxidation." In the case of steel, iron dissolves to form either ferrous (Fe^{2+}) or ferric (Fe^{3+}) cations, depending on the environmental conditions. The cathodic reaction involves a gain of electrons, and is referred to as "reduction." In the case of steel, the cathodic reaction is typically the reduction of oxygen, if the environment is aerated, or reduction of water if the environment is deaerated. In acidic environments, hydrogen ions may be reduced and gas evolved. The two electrochemical half reactions occur in parallel.

Pipelines are typically protected from corrosion by both corrosion resistant coatings and impressed current cathodic protection (CP) systems. The corrosion resistant coating provides a barrier to water, which is necessary to act as an electrolyte to support the corrosion reactions and to provide the chemicals necessary to drive the reactions. All coatings contain defects, referred to as holidays, and corrosion can potentially occur at these defects. Coatings degrade with time and the population of defects increases with time. CP prevents corrosion at these coating holidays. The CP system takes advantage of the electrochemical nature of the corrosion reactions. The system provides excess electrons to the pipe steel surface, in effect counter-acting the natural tendency of the steel to corrode. In addition to coating defects, corrosion may also occur when electrolytes are present under disbonded coating, where cathodic protection is shielded from reaching the pipe steel surface. If a pipeline is removed from service and abandoned in place, the CP system may also be removed from service. This allows the natural corrosion reactions to occur. However, corrosion will only occur at areas of damaged coating, where water is in direct contact with the pipe surface.

3.1.2 The Soil Environment

Corrosion of steels in soils is a complex phenomenon, due to the many factors that contribute to corrosion and the many varieties of soil that exist in nature. Figure 1 is a schematic of a pipeline buried in soil, illustrating the local environment. The pipe surface is surrounded by soil. If the pipe is below the water table, then water is in direct contact at all times. If the pipe is above the water table, the pipe is only in contact with water from "gravitational" water from surface run-off or precipitation. The pipe surface is also surrounded by oxygen, either dissolved in the water or diffusing into the soil from the surface. The dissolution of carbon dioxide in water can also be an important contributing factor in the development of corrosion. Given the importance of water, oxygen, and carbon dioxide to the corrosion reaction, it is important to corrosion rate predictions that the environment is well understood.

Soils can be classified as organic or inorganic. Organic soils are found in peats, bogs, and swamps, and so have a high water content. They consist of decaying organic matter and inorganic matter weathered to various particle sizes. Inorganic soils consist primarily of the inorganic matter and are generally classified by their particle size. Coarser soils are referred to as "sands", moderate soils as "silts" and finer soils as "clays." Soils with a range of particle sizes are referred to as "loams." Figure 2 is a ternary diagram describing soil types by their characteristic particle sizes [18].

The particle size has an influence on the corrosion rate of steel due to the soil permeability. The coarse sands have a higher permeability, allowing oxygen and water to flow easily. This allows water to drain away from the pipe surface and allows oxygen to replenish during the corrosion reactions. The fine clays have lower permeability, decreasing flow rates of both water and oxygen. The fine pores may lead to capillary action, drawing water into the clays. Soils become waterlogged, decreasing the available oxygen. This leads to anaerobic conditions.

The mineral contents of the soils tend to trend with the particle sizes. Coarse sands consist of quartz, carbonates and feldspars. Finer soils consist of feldspars, mica and mineral clays. Quartz soils tend to be inert. Soils formed from limestones and dolomites contained dissolved carbonates, which tend to buffer electrolytes to alkaline conditions. This allows passive layers to form, which protects the underlying steel from further damage. Carbonates may precipitate scales on pipe surfaces and decrease corrosion rates. Soils containing fine mineral clays have higher surface energies per unit volumes that coarser soils and this has an effect on electrochemistry at the particle-water interfaces.

Climate can also affect soil composition. Arid, tropical, temperate and arctic regions have different precipitation. This affects the dilution and precipitation of various salts, and can affect the acidity or alkalinity of the soil. In addition, the temperature can have a significant influence. Temperature not only affects the rate of chemical reactions, but can also affect the chemistry of the soil. Cold conditions in arctic environments can freeze water, segregating salts and creating highly saline regions.

As discussed above, there is a diverse range of possible soil types. Soils differ by organic content, moisture, particle size, mineral content and salt content. These differences must be considered to predict the corrosion rates of steels in various soils.

3.1.3 Corrosion Rates in Soil

Water and oxygen both play key roles in the corrosion reactions. Dry soils are typically not of concern for corrosion. Wet soils are of concern, and the water content can influence the corrosion mechanisms. Soils with low water contents (<20%) are subject to pitting corrosion, whereas soils with higher water contents (>20%) are subject to general corrosion [6]. However, if water saturates the soil, oxygen availability is decreased, and corrosion conditions might change from aerobic to anaerobic conditions. The cathodic reactions supporting the process change from oxygen reduction to water reduction. This affects the acidity or alkalinity of the environment. Table 1 is a classification of corrosivity based on drainage [11].

In some cases, there is variation in aeration and moisture content in different areas of the pipeline. This can lead to the development of macro-cells. If one area of the pipeline is anodic relative to another (cathodic) area of the pipeline, then a corrosion cell is formed. For example, this may occur if the top of the pipe is dry and aerated, and the bottom of the pipe is wet and deaerated. In this case, the cell drives corrosion on the bottom of the pipe. The most severe corrosion occurs under these conditions and is reflected in the corrosivity classifications shown in Table 1.

The pH is a measure of the acidity or alkalinity of the soil. Lower pH soils (~ 4) are acidic. Corrosion rates of steel are typically higher, as the acid dissolves protective films that form on the metal. If the pH is low enough, the metal dissolves and the reaction evolves hydrogen. The evolution of hydrogen removes hydrogen ions from the solution and raises the local pH. Higher pH soils (~ 10) are alkaline. Corrosion rates are typically low, as the hydroxides in the water precipitate to form protective, or "passive", layers on the metal surface. Neutral, or near-neutral pH soils (~ 6 to 8) have moderate corrosion rates. The corrosion rates are sensitive to the ion contents, oxygen availability and resistivity of the water and soil.

Soil resistivity is another way to categorize soil corrosivity. Lower resistivity typically is associated with higher concentrations of corrosive anions, such as chloride, and leads to severe corrosion; whereas, higher resistivity leads to milder corrosion. Table 2 is a classification of corrosivity based on resistivity [41]. Table 3 provides typical resistivity ranges for various soil types and water types [11].

King [8] developed a nomogram to relate the pH and resistivity to corrosion rates of steels, see Figure 3. It allows one to estimate a pitting rate (in mm/year) and a weight loss ($g/m^2/year$) as a function of resistivity and pH. The nomogram does not consider the electrical potential or the role of microbial activity.

The relationship between ion content and soil corrosivity is not direct. Some ions have additional effects on corrosion mechanisms that influence corrosion rates. For example, the presence of calcium (Ca^{2+}) or magnesium (Mg^{2+}) cations can decrease corrosion rates by precipitating carbonates and forming passive steel surfaces. The presence of chlorides (Cl^{-}) or sulfates (SO_4^{2-}) can lead to more severe corrosion of bare steel surfaces. Chlorides destabilize protective films and can results in pitting of the steel. While Table 1 and Figure 3 can be used as guidelines, they are not directly applicable to all soil environments.

The corrosivity of a soil can also be estimated by the oxidation-reduction potential. In aerobic conditions, the oxygen content of the soil is high, leading to higher potential and lower susceptibility to corrosion. In anaerobic conditions, the lower potential leads to higher susceptibility. Table 4 is a classification of soil corrosivity based on oxidation-reduction potential [7]. As described above, variation in aeration of soils on different parts of the pipeline can lead to macro-cells. Deaerated areas, such as lengths of pipe under roads, become anodic relative to aerated areas, and this drives corrosion in the deaerated areas. In addition, it should be noted that the application of CP systems leads to beneficial low potentials by artificially drawing the potential of the pipeline down and forcing cathodic reaction on the steel surface.

Another factor that may play a role in corrosion of pipeline steels is the presence of microbes. Various types of microbes are known to contribute to pipeline corrosion reactions. Two of the more common types that contribute to corrosion of buried pipelines are acid producing bacteria (APBs) and sulfate reducing bacteria (SRBs). Both types of bacteria may be present in organic soils. APBs have metabolisms that produce acid and contribute to corrosion by decreasing the pH of the local environment. The acid dissolves the steel. SRBs have metabolisms that reduce sulfates in the environment to form hydrogen sulfide. Sulfate reduction is more common in anaerobic environments.

3.1.4 Culvert Service Life Prediction Models

Several states' departments of transportation have developed corrosion rate models to estimate the service live of culverts. They are based on a chart developed by the California Department of Transportation in 1972 [11]. The chart was compiled from corrosion rate data derived from the inspection of over 7,000 culverts. The basic form is illustrated in Figure 4.

The California DOT method bases its service life predictions on the pH and resistivity of the soil. The soil properties are considered representative of the ground water in the culvert. Two models are included in the chart, one for acidic soils and one for neutral or alkaline soils, specified as pH >7.3. For the acidic soils, service life increases with increasing resistivity and increasing pH. The relationship between service life and environment is described by:

Equation 1: $$SL_b = 17.24 \cdot [logR - log(2160 - 2490 \cdot logpH)]$$

where:

SL_b service life in years (base)
R resistivity (Ωcm)

The base service life assumes a 16 gauge steel culvert (that is, 1/16 inch, or 1.59 mm). If a thicker gauge is used, a multiplication factor is applied to the base service life. The multiplication factor can be approximated as linear with gauge thickness, but some researchers [11] have proposed a power law relationship, as the corrosion rates are observed to decrease with time for the thicker gauges. If the steel is coated, a constant service life length is added to the estimate. The constant varies for different coating types.

For neutral to alkaline soils (pH >7.3) a different relationship is used:

Equation 2: $$SL_b = 1.84 \cdot R^{0.41}$$

Both the acidic and alkaline relationships are illustrated in Figure 4.

The California DOT model is based on the "service life" which requires a clear definition. Two levels of corrosion damage are defined; (a) the time to first perforation, and (b) the time to loss of function. The time to first perforation has been statistically correlated to an average thickness loss of 13%. The time to loss of function is defined as an average thickness loss of 25%, so approximately twice the time to perforation.

The California DOT model has been statistically analyzed and shown to be approximately valid [11]. However, service lives vary ±10 years from the models predictions. Several other state authorities (Arizona, Colorado, Utah) and industry associations (American Iron and Steel Institute) have offered modifications to the basic model. The AISI model predicts service lives twice as high as the California DOT model, and is generally considered as non-conservative.

It is important to recognize that the culvert models developed and used by the various state DOTs are based on the assumption that the culverts have water and air flowing through them during their service lives. The corrosion of interest is primarily internal corrosion, due to water flow through the culvert, though corrosion may be present on both the internal and external surfaces of the culvert. In the case of abandoned oil and gas pipelines, it is assumed there is minimal water on the inside of the pipeline. If the ends are capped, then no water or air flows. Water may accumulate in pipelines if perforated by corrosion, but this is likely to be a minimal amount and will not occur until many years after the pipeline has been abandoned. There is minimal oxygen present and this restricts the corrosion reactions.

The corrosion of interest to abandoned pipelines is external corrosion. Pipelines typically have a corrosion resistant coating on the outside, and these coatings may degrade with service and time. However, industry estimates are that the area of disbonded coatings is of the order of one percent of the pipe surface. This means that only one percent of the external surface of the pipe is subject to corrosion. This suggests the culvert models would be extremely conservative if used as life prediction models for pipelines.

3.1.5 National Bureau of Standards Test Data

The (US) National Bureau of Standards (NBS) initiated an extensive series of tests in 1922 to measure corrosion rates of various metals and alloys in a number of soil environments. The results of the eighteen year study (1922-1940) were published by the NBS in 1957, and later by the National Association of Corrosion Engineers (NACE) in 1989 [17].

The NBS program involved burying various metals and alloys in the soils for extended periods of time. Multiple test samples were buried at each location. At pre-determined time intervals, one sample was retrieved from each test site, with the remaining samples left in place. The test samples were weighed to determine mass loss, and maximum penetration depths were measured. The resulting data was tabulated for reference. The study is one of the largest and most comprehensive programs ever performed to measure corrosion rates in soils.

The metals and alloys studied included several ferrous alloys, including wrought and cast irons, plain carbon steels and low-alloy steels. The NBS report provides manufacturing process and chemistry of each alloy.

The soils studied were the native soils in over 150 test sites from around the United States. The soils were analyzed for chemistry. Measurements included pH, total acidity, and the concentrations of sodium, potassium, calcium, magnesium, carbonate, bicarbonate, chloride and sulfate ions. The resistivities of the soils were measured. The local climatic conditions were recorded.

The NBS report provided simple numerical analyses to quantify the corrosion rates. Linear regression analyses were performed on data sets to confirm that data fit an equation in the general form:

Equation 3: $$d = k \cdot T^n$$

where:

d	depth of penetration of the deepest pit
k	curve fit coefficient
T	time
n	curve fit coefficient

Several other researchers have also used this general form of equation in describing corrosion rates [19-25].

The National Institute of Standards and Technology (NIST, formerly the NBS) performed more rigorous statistical analyses more recently, in 2007 [18]. The analyses identified several trends in the data, but the uncertainties associated with the calculations were significant. The analysts concluded that an “estimation of corrosion damage distributions and rates can be developed from these data, but these models will always have relatively large uncertainties that will limit their utility.” Figure 5 is a selection of plots prepared during the statistical analysis of the NBS soils corrosion data. Without going into detail on the different types of corrosion rate measurements, the significant scatter evident in the data indicates the difficulty in developing accurate models.

3.2 Structural Integrity of Buried Pipelines

Predicting the structural integrity of an abandoned buried pipeline requires understanding of the behavior of both the soil and the buried pipeline. Soil has several properties that are important to the corrosion of the underlying steel pipe surface, as discussed above. Soil pH, water and oxygen content, and salt content influence to corrosion rates. For the soil mechanics component of the modelling, the soil density, cohesion, modulus and bedding factor become important. These properties depend, in part, on the soil type, environment, and how the pipeline was installed during construction. The pipeline also has properties that differ for the corrosion and structural integrity modelling components. For the corrosion modelling, only the wall thickness is considered. For the structural integrity modelling, the diameter and pipe material are important. The pipe steel, and any coatings or liner on the pipe, must be considered.

The behaviour of soils subject to loads is described by soil mechanics. The properties are highly dependent on the type of soil (sand, silt, clay, etc.), and the water content. The coarser and drier soils, for example, desert sands, tend to have more fluid-like properties. The soils do not resist mechanical loads in shear, and this allows the particles to move and the soil to flow. The finer and wetter soils are more able to resist the shear and are more rigid. These properties will affect how surface loads are transferred to a buried pipeline, and how the soils are able to move to accommodate deformation of the pipeline.

The primary load acting on an onshore service pipeline is typically the internal service pressure. The internal pressure results in significant tensile stress acting in the plane of the pipe wall. Pipelines are designed to withstand this service pressure by use of appropriate steel grade and wall thickness. The design requirements are well established, and used as the basis for various industry standards. However, the stresses acting on an abandoned pipeline are not due to internal service pressure.

The first load to consider acting on an abandoned pipeline is the weight of the soil above the pipeline. The density and the water content of the soil are important, as is the depth of cover. The higher the density of the soil and greater the depth of cover, then the greater the pressure acting on the top of the pipe. The load will act directly downward on the pipe, and lead to ovalization of the pipe.

Two other important factors can influence the pressure acting on the pipe; the height of the water table, and how the pipeline was installed during original construction. If the water table is above the pipe, then a buoyancy force acts on the pipe. This has the effect of reducing the effective load over the pipe. If a pipe is jacked into place rather than using the conventional construction of trenching and laying, this must also be considered. The undisturbed soil has the effect of self-support and this decreases the load acting on the pipe.

The second type of load that must be considered is “live” load acting on the ground surface. Live loads may refer to anything acting on the surface; people, vehicles, equipment, or animals. The pressure experience by the pipe is not equivalent to the pressure acting at the ground surface. The pressure at the ground surface is dissipated below the surface. The degree of dissipation depends on soil properties, the depth below the ground surface, and the horizontal location. So, for example, if we consider the weight of a truck on the ground surface , we must consider the depth of cover of the abandoned pipeline below, and we must consider whether the truck is directly “over” the pipeline, or “near” the pipeline. These subsurface pressures can be calculated using established equations [26, 36].

The sub-surface pressures associated with surface loads are of particular interest to this program. The effect of surface loads, are in general, much more significant than the pressures associated with soil loads. The pressures due to vehicles traffic over the pipeline may be significant. In fact, in some cases the soil loads can be neglected.

Pressure above the pipeline will lead to ovalization of the pipe. This may lead to either plastic collapse or elastic collapse of the pipe. Plastic collapse occurs when the bending stress acting on the pipe wall exceeds the yield strength of the pipe material. This form of collapse uses yielding strength (N/m^2) of the pipe material as the critical point. The use of yield stress is conservative. The effects of strain hardening, and stress distribution throughout the pipe wall on the yield strength are not considered in this analysis. When the yield strength of the pipe wall is exceeded, the wall yields and the pipe can no longer support the loads acting on the top of the pipe. Plastic collapse is explained in further detail in Section 5.3 of this report.

Elastic collapse, or "buckling", occurs when the elastic energy (N m) in the pipe wall due to loads acting from above exceed a critical value. The pipe reduces its internal elastic strain energy by collapsing in on itself. The two failure modes must be considered during the development of any structural integrity models. Elastic collapse is explained in further detail in Section 5.4 of this report.

The ovalization of the pipe wall can be quantified by the deflection of the top of the pipe from its original locations. Equations to describe the deflection were developed by Professor Spangler at Iowa University in the 1940's, and are often referred to as the "Spangler Equation" or "Iowa Equation". The equations calculate the vertical deflection of the pipe as a function of the applied load, the pipe diameter, wall thickness and material, the modulus of soil reaction, the lag factor and the bedding constant. The lag factor and bedding factors are empirically derived constants that depend on how the trenching is performed during laying of the pipe. Several modifications have been proposed over the years to account for the inherent assumptions in the original equations [36, 40].

The critical buckling load can also be quantified by established equations [36]. Elastic collapse is a function of the pipe diameter, wall thickness and material, the modulus of soil reaction, and an empirical coefficient of elastic support. The empirical constant is a function of pipe diameter and depth of cover.

The various equations that have been developed over the years that relate to structural integrity will be discussed in further detail below. These equations are used as the basis of the structural integrity models.

4.0 CORROSION MODELLING

The objective of the corrosion modelling is to determine the extent of corrosion damage to the pipeline as a function of soil environment and time. The literature review above identified two possible options to provide the basis of a corrosion model; the California DOT based culvert life prediction model, and the extensive NBS soils corrosion data. A primary difference in the two models is that the California DOT model is primarily based on internal corrosion, and the NBS corrosion data is based on external corrosion.

The California DOT culvert life prediction model was identified by the NEB gaps analysis [5]. It provides a "ready-made" model, which could, in principle, be applied to this pipeline abandonment study. However, several issues should be considered, as discussed above. In particular, the culvert model is tacitly based on internal corrosion, as opposed to the external corrosion, which is a more likely threat to an abandoned pipeline. If a pipe becomes perforated after many years of abandonment, the water may accumulate at the 6 o'clock orientation and the culvert model may become applicable.

The environment on the external surface of the abandoned pipeline will be soil. Oxygen, water, and carbon dioxide can be replenished to sustain the corrosion reactions, though not as quickly as flow through a culvert. The properties of the soil and the local weather will determine the rates. The NBS measurements provide more realistic conditions to calculate the corrosion rates on the external surface of the pipeline. The NIST statistical analyses indicated there were unclear correlations between corrosion rates and the various soil properties, and this must be considered in the modelling.

The NBS study performed tests on over 150 test sites around the United States. Of these, forty-seven test sites were selected for more detailed study. Their native soils were particle-size analyzed and characterized using a classification system similar to that provided in Figure 2. Data for these forty-seven soils are provided in Table 5 and Table 6 . Analysis of these data allows a simple corrosion model to be developed in which the corrosion rate is estimated based on the basic soil properties.

It is of interest to this study to consider how the corrosion rates measured during the NBS program compare to the California DOT culvert model. In particular, it is of interest to compare how the measured corrosion rates trend with both acidity (pH) and resistivity of the soil.

Figure 6 and Figure 7 are plots of the NBS data (from the forty-seven test sites of detailed study) as a function of acidity and resistivity, respectively. In each plot, two sets of data are considered. The first set of data is based on the mass loss measured during the NBS study. The mass loss was used to estimate a depth of corrosion, assuming uniform corrosion. The second set of data is the maximum penetration depth measured during the NBS study. The data shown here all correspond to measurements on samples that were retrieved from their respective tests sites after approximately twelve years of burial. The two figures indicate that there is no clear trend between the corrosion rates and the acidity or the resistivity. There is a slight trend observed in the resistivity, but not significant enough to use resistivity as the basis of an accurate corrosion rate model. This is true for both the mass loss calculation and for the penetration depth measurements.

Figure 8 is a plot of the NBS penetration depth data as a function of the predicted service life, as predicted by the California DOT culvert model (Equation 1 and Equation 2). No adjustments have been made to account for a given wall thickness. The figure is intended only to demonstrate any trend in the data. The figure does indicate an inverse proportionality between penetration depth and service life, as expected. While the trend in the data does show general agreement between the NBS data and the culvert model, there is notable scatter in the data.

The NBS data were plotted in several ways during the course of the analysis, and it was demonstrated that there is also a weak, but useable, correlation between the mass loss data and the internal drainage of the soil. This is consistent with the relative corrosivity ranking shown in Table 1. Soils with very poor drainage, such as peats and marshes, tended to have higher mass loss rates. Soils with good drainage, such as sandy loams, tended to have lower mass loss rates. This is consistent with the soil classification based on potential, as shown in Table 4. There was one clear exception to the trend, with Soil #23 in Table 5, a soil with fair drainage had the highest mass loss of all the soils tested. The reason for this is not clear. However, it was noted that this soil was the only significantly alkaline soil (pH 9.4).

Figure 9 through Figure 12 are plots based on the mass loss data from the NBS study for uncoated steel samples. In each case, the mass loss data were used to estimate a depth of corrosion, assuming uniform corrosion, as described above. These calculated data were plotted as a function of the time of sample exposure. A curve is included in each plot that provides a "reasonable" upper bound to the data. Soil #23 is a clear exception to the curve shown in Figure 11.

The curves shown in the figures were fit using engineering judgment, rather than any rigorous mathematical techniques. The form of the equation used for the fits was Equation 3. In each case, there was a reasonable upper bound fit to curves with an exponent of ½. Visual examination of the curve indicates the assumption of ½ is realistic, and would provide conservative corrosion depth estimates at long times. Other exponents and coefficients could be used in the modeling if site specific data indicate that they would be more appropriate. For example, these corrosion data were obtained from uncoated specimens and higher corrosion rate kinetics may be associated with disbonded coatings on specimens.

A similar methodology was applied to the penetration depth data. However, the trend was not as clear as with the mass loss data. The penetration depths from the four drainage categories were less sensitive to drainage. Figure 13 through Figure 16 are plots of the penetration depth data as a function of time. As with the mass loss data, upper bound curves are provided, with exponents of ½, also based on engineering judgment. There is significantly more scatter in the penetration data than for the mass loss data.

It is of interest to compare the mass loss data with the penetration rate data from the NBS study. Figure 17 is a plot of the penetration depth data as a function of the corrosion depth based on mass loss. There is a general trend that the penetration depth increases with mass loss, as would be expected. The ratios of the depths of penetration to corrosion based on mass loss vary between three and twenty-five. The majority of these penetration ratios are between five and ten.

Figure 18 is a plot of the penetration ratio as a function of corrosion depth based on mass loss. Note that the mass loss data showed the clearer trend with drainage than did the penetration depth data. In this case, there is an inverse trend between penetration ratio and mass loss. The soils with lower mass loss tended to have a higher penetration ratio. These were the soils with "good" internal drainage. The higher ratio indicates more localized corrosion damage, that is, pitting. The soils with the higher mass loss tended to have a lower penetration ratio. These were the soils with "poor" or "very poor" internal drainage. The lower ratio indicates more uniform damage, which is more relevant to this project.

Table 7 list the coefficients and exponents used for the curves provided in Figure 9 through Figure 16. In each case, the curve is in the form of Equation 3. While these coefficients and exponents were not derived through rigorous mathematical techniques, they do provide simple and reasonable bounds to the data, and can be used for corrosion rate estimates. A penetration ratio is also provided in the table.

In some cases, the use of an upper bound corrosion rate may be considered too conservative. A less conservative approach would be to decrease the "k" coefficient. A value of one-half of the coefficients given in Table 7 could be considered an "average" value, rather than an upper bound. This approach should be considered with discretion. As described above, other exponents and or coefficients could be used in the modeling if site-specific data indicate that they would be more appropriate. For example, these corrosion data were obtained from uncoated specimens and higher corrosion rate kinetics may be associated with disbonded coatings on specimens.

Pipeline wall thickness decreases as an abandoned pipeline corrodes. As the wall thickness decreases there is a change in the load bearing capacity of the pipeline. This will be discussed in detail in the following section. However, it is important to consider both the mass loss and penetration depth data to determine how to predict the effective corrosion damage to the pipeline with time.

A simple approach to determining the corrosion damage to the pipeline is to use the mass loss data, and predict the depth of corrosion as a function of time, assuming uniform corrosion. However, this approach will be non-conservative in predicting the time to penetration of the wall thickness. The other option would be to use the penetration depth data, but this would be overly conservative in predicting the overall corrosion damage to the pipeline. A balance of these two approaches is necessary.

Consider the penetration ratio and the effective area that is corroding. A soil with a higher penetration ratio has a lower effective area that is corroding, but at the higher penetration rate (rather than the lower mass loss rate). If a given soil has a penetration ratio of ten, for example, then one could reasonably consider this as corrosion of only $(^1/_{10})^{th}$ of the area, but at the penetration rate. This is a simple geometric argument that balances the conservatism of the two, more extreme, options.

Regardless of whether the mass loss or penetration rate approach is considered more suitable, the thickness of the pipe wall can be estimated as a function of the initial or nominal wall thickness, the time and the corrosion model coefficients. To estimate the remaining thickness of pipe:

Equation 4: $$t = t_0 - k \cdot T^n$$

where:

t	remaining wall thickness of pipe
t_0	initial or nominal wall thickness of pipe

This model applies to both mass loss and penetration. The mass loss is considered more applicable to the structural integrity modelling, as it is indicative of overall damage. The penetration is of interest in determining when water might first enter the pipeline.

For example, consider a pipe with a nominal wall thickness of 6.35 mm, buried in soil with "poor" drainage for 50 years. For soil with poor drainage, and assuming uniform corrosion loss, we will use the upper bound k_{ml} = 0.15 and n = 0.5.The remaining wall thickness is estimated as:

$$t = 6.35 - 0.15 \times 50^{0.5} = 5.3\ mm$$

Note that the corrosion is not uniform, and so this should be considered as an average remaining wall thickness.

It is also of interest to estimate the time to penetrate the pipe wall, or the time to corrode the pipe to "zero" wall thickness:

Equation 5: $$T_p = \left(\frac{t_0}{k}\right)^{(1/n)}$$

where:

T_p time (in years) to penetrate full wall thickness of pipe steel

Consider the same example pipe as described above. In this case, we will estimate the time to penetrate the pipe wall, and use the upper bound k_p = 1.0 and n = 0.5. The time to penetrate is estimated as:

$$T_p = \left(\frac{6.35}{1.0}\right)^{(1/0.5)} = 40\ years$$

Note that because the corrosion is not uniform, the pipe wall may be penetrated while the equivalent uniform mass loss is relatively low. The relation will be more extreme for the soils with the higher penetration ratios, that is, the soils with good drainage.

Consider a pipe of wall thickness 9.5 mm, subject to varying corrosion rates. Consider an "average" soil with good drainage and k_{ml} = 0.025 mm/√yr, an "upper bound" soil with fair drainage and k_{ml} = 0.10 mm/√yr, and Soil #23 with k_{ml} = 0.25 mm/√yr. Figure 19 is a plot of calculated wall thickness as a function of time. The curves are based on Equation 4. The plot demonstrates that loss of pipe wall, based on uniform corrosion, takes several hundreds, or thousands, of years for a relatively thick pipe for the assumed coefficients and exponent. Shorter times to perforations would be calculated for larger assumed coefficients and exponent.

Perforation of the pipe wall will allow ground water and precipitation to seep into the pipeline, and this will allow for internal corrosion. Water will likely drip in from holes at the top of the pipe and accumulate at the 6 o'clock orientation. In this case, the culvert model may become more applicable. Note, however, that rainwater dripping into the pipeline will be significantly less than water flow through a culvert, the pipe wall is typically multiple times thicker than the culvert material, and the basic culvert model does not account for the diminishing corrosion rates observed in service. While these considerations support the idea that the culvert model is conservative, the corrosion mechanism in the perforation scenario is likely different than that in the culvert (i.e., flowing water) scenario.

It should be noted that these corrosion rates are only applicable to areas of disbonded coating on the pipeline, which will increase with time. An intact coating excludes water from the pipe surface and prevents all forms of corrosion. After many years, the disbonded areas will corrode through-wall. The result will be a pipeline with a "Swiss cheese" character. The coated areas will remain intact, but there will be dispersed holes corroded through the pipe wall at the areas of coating disbondment. In the analyses described in Section 5.5, disbonded areas of 1% and 10% are considered. The former would represent a high quality coating such as fusion bonded epoxy while the latter would represent a poorer quality coating such as asphalt. The quality of the coating must be considered in the structural integrity modelling efforts.

5.0 STRUCTURAL INTEGRITY MODELLING

The objective of the structural integrity modelling is to determine the load bearing capacity of the pipeline as a function of corrosion damage. As a pipeline corrodes, the wall thickness decreases or the pipeline becomes perforated, and this changes the pipeline's load bearing capacity. The load bearing capacity will therefore change with time. It is possible to determine the critical surface load necessary to cause collapse for a given pipe geometry and soil conditions. In combination with the corrosion rate modelling, it is possible to determine the critical surface load as a function of time, or the time to collapse due to soil weight alone.

The first step in the structural integrity modelling is to determine the loads acting on the pipe. As the pipeline is abandoned, there is no internal service pressure. The load acting on the pipe is the static vertical pressure due to the weight of soil above the pipe and the weight of any "live" loads over the pipe. Live loads refer to vehicle traffic, equipment, people, or animals. The loads act vertically downwards and lead to ovalization of the pipe. Figure 20 is a schematic of the parameters used for the basic soil models developed below.

5.1 Soil Loads

The vertical load on the pipe due to the weight of soil above is referred to as the "prism load". The prism load depends on the density of the soil and the depth of cover [36]:

Equation 6: $$P_{soil} = \gamma_s \cdot C$$

where:

P_{soil}	soil pressure acting on top of the pipe (Pa)
γ_s	dry density of soil (N/m^3)
C	height of soil above pipe (m)

Note that the density is a weight density, rather than a mass density. If metric units are used, and the soil density is reported as mass density, such as g/cm^3 or kg/m^3, the mass density must be multiplied by the gravitational constant of 9.8 m/s^2. If imperial units are used, no correction is required as the "pounds-per-square-inch" typically reported is a weight density. If an imperial mass density is reported (ie. slugs) then a gravitational constant of 32 ft/s^2 must be included.

The above equation assumes the pipe is buried above the water table. If the pipe is buried below the water table, a correction must be applied to the pressure calculation. The weight of water above the pipe also provides downward pressure acting on the pipe. However, the water also provides a buoyancy force that acts upward on the pipe. The net pressure acting on the pipe is calculated by including the weight of the water above the pipe and a "water buoyancy factor" into Equation 6 [36]:

Equation 7: $$P_{soil} = \gamma_w \cdot h_w + R_w \cdot \gamma_s \cdot C$$

where:

γ_w	density of water (N/m^3)
h_w	height of water table above pipe (m)
R_w	water buoyancy factor

and

Equation 8: $$R_w = 1 - \frac{1}{3} \cdot \left(\frac{h_w}{C}\right)$$

The density of fresh water is taken as 1000 kg/m^3, which corresponds to 9.8 x 10^4 N/m^3. If imperial units are used, the density of fresh water is 62.4 lb/cf.

The above equations assume the pipe is buried in disturbed soil. A trench is excavated during construction, the pipe is laid in the trench and the pipe is covered with back-fill. The pressure acting on the pipe amounts to the full weight of the back-fill soil. However, in some situations the pipe is installed into the soil by jacking. The undisturbed soil provides more support due to soil cohesion and friction, and the load acting on the pipe is decreased. For a pipe in undisturbed and unsaturated soil [32]:

Equation 9: $$P_{soil} = \gamma_s \cdot C - 2 \cdot \lambda \cdot \left(\frac{C}{D}\right)$$

where:

λ	soil cohesion (Pa)
D	outside diameter of pipe (m)

Soil cohesion ranges from 0 Pa for dry loose sands, to approximately 70 kPa for hard clays.

When pipe diameter is used in calculations, the original, un-corroded, outside diameter is used regardless of degree of wall loss due to uniform corrosion.

Inspection of Equation 9 indicates it is mathematically possible to have a negative load acting on the pipe. In such circumstance, it should be taken that the soil fully supports the loads and the pressure due to the soil be taken as zero.

5.2 Live Loads

The vertical load on the pipe due to the weight of traffic or equipment on the ground surface is referred to as the "live load." The live load acting on the top of the pipe depends on the magnitude of the applied load on the ground surface, the depth of cover, and horizontal distance between the applied load and the pipe centre line [26, 36]:

Equation 10:

$$P_{pipe} = \frac{3 \cdot P_{live} \cdot F'}{2 \cdot \pi \cdot C^2 \cdot \left[1 + \left(\frac{h}{C}\right)^2\right]^{5/2}}$$

where:

- P_{pipe} pressure acting on top of pipe due to live point load (Pa)
- P_{live} live point load at the ground surface (N)
- F' impact factor
- h horizontal offset distance between applied point load and pipe centre line (m)

Note that the load acting on the top of pipe is calculated as a pressure in units of Pascals (Pa), whereas the live load acting on the ground surface is a force in units of Newtons (N).

Because Equation 10 requires a live point load, the horizontal offset distance between applied point load and pipe centre line must be determined based on an assumed "point" location for the surface load. The location of the applied point load could vary depending on the type of surface load.

The impact factor is included to account for irregularities in the ground surface. Table 8 is a listing of impact factors that can be applied to truck traffic, railways and airports [36].

Equation 10 calculates the effective pressure acting on the top of a buried pipe due to a point load force acting on the ground surface. When a distributed load acts on the ground surface, Equation 11 can be used to calculate the effective pressure acting on the top of a buried pipe.

Equation 11: $$P_{pipe} = q\frac{1}{\pi}\left[\left(\frac{2mn\sqrt{m^2+n^2+1}}{m^2+n^2+m^2n^2+1}\right)\left(\frac{m^2+n^2+2}{m^2+n^2+1}\right)+\tan^{-1}\left(\frac{2mn\sqrt{m^2+n^2+1}}{m^2+n^2-m^2n^2+1}\right)\right]$$

where:

q	live load pressure acting on surface (Pa)
m	(B/2)/C
n	(L/2)/C
L	length of rectangular area load (m)
B	width of rectangular area load (m)

Equation 11 is the integration of Equation 10, and can only be used in this form to calculate the effective pressure acting on the pipe when the surface load is directly centered over the pipe. This equation is useful when the surface loads are high, and the weight is distributed over a larger area such as in the case of agricultural equipment.

Calculations have been performed by the civil engineering industry, using the above Equation 10, to determine the effective loads acting on the top of a pipe for various vehicles, including highway trucks, rail, and aircraft [36]. Table 9 is a listing of effective loads transferred by the various vehicles to buried pipe as a function of vehicle type and depth of cover. This allows for a simple "look-up" table for effective pressures acting on a buried pipe due to vehicle traffic. This table was recreated from Reference [36] and loads are reported in imperial units.

Table 10 is a copy of Table 9 with two differences. The first is that metric units are used. The units used in Table 10 are metres (m) for the depth of cover, and kilopascals (kPa) for the effective pressure acting on the top of the pipe. The second difference is that two columns have been added. Column 5 provides an effective pressure acting on top of a pipe due to a personal truck on the ground surface. Reference [36] provides data assuming a 20-ton commercial truck driving along the highway. Table 10 Column 5 considers a 5-tonne personal truck driving across a pipeline right-of-way. The data in the column is based on a simple ratio of truck weights. It was not derived from first principles and so is subject to the assumptions of the original calculation and the simplification that the truck weights scale directly. Column 6 provides an effective pressure acting on top of the pipe due to a person standing on the ground surface. Table 10 Column 6 assumes a person of 100 kg mass standing directly over the pipeline. Equation 10 was used to perform the calculations and no impact factor was used.

5.3 Plastic Collapse Model

Pressure acting on top of the pipe due to soil and live loads will lead to ovalization, illustrated schematically in Figure 21. The degree of ovalization is a function of the loads acting on the top of the pipe and the properties of both the pipe and soil. The vertical deflection of the top of the pipe can be determined using the modified Iowa equation [36]:

Equation 12: $$\frac{\Delta y}{D} = \frac{L \cdot K \cdot (P_{soil} + P_{pipe}) \cdot R^3}{(EI)_{eq} + 0.061 \cdot E' \cdot R^3}$$

where:

Δy	vertical deflection of top of pipe (m)
L	lag factor (~ 1.0 to 1.5)
K	bedding constant (~ 0.1)
R	radius of pipe (m)
$(EI)_{eq}$	equivalent stiffness of pipe wall per unit length (Nm)
E'	modulus of soil reaction (Pa)

The lag factor is an empirical constant measured in the field. A lag factor of ~ 1.5 is considered conservative. The bedding constant is a function of the bedding of soil below the pipe at the time of construction. A bedding constant of ~0.1 is appropriate for a pipeline constructed by trenching and back filling. The modulus of soil reaction is a function of the soil type and the compaction of the soil. Table 11 and Table 12 are listings of appropriate design values for soil modulus, in imperial units from Reference [29], and converted into metric units, respectively.

Note that in this form of the equation the loads used are *pressure* loads, as defined above in Equation 6 through Equation 10. Alternate forms of the equation are available in the literature that use *weight* loads, and in these cases, the deflection calculated is an absolute deflection ("Δy"), rather than the relative deflection ("Δy/D") provided above. The two forms of the equation are both mathematically valid. The above form of the equation has been used as it allows the relative deflection to be used directly in the bending stress calculation discussed below, and it allows literature values for the loads associated with vehicular traffic to be more easily included, also discussed below.

The equivalent stiffness of the pipe wall per unit length is a function of the components of the pipe wall and their elastic properties and thicknesses. It is considered that any pipeline may have an external coating and an internal liner. The external coating may be a corrosion resistant coating or a concrete casing. The internal liner is typically a corrosion resistant coating. The equivalent stiffness of the pipe wall per unit length is given by [36[1]]:

Equation 13: $$(EI)_{eq} = (EI)_{pipe} + (EI)_{coat} + (EI)_{line}$$

where:

E	modulus of pipe steel, coating or lining (Pa)
I	second moment of area (per unit length) (m^4/m)

1 This equation is provided as reported in Reference [36]. However, the equation includes simplifications and should be used with caution if the pipeline has a coating or liner with significant stiffness or thickness.

The subscripts represent the pipe wall, the coating and the liner, respectively. The second moment of area per unit length is given by:

Equation 14: $$I = \frac{t^3}{12}$$

where:

t wall thickness of pipe steel, coating or lining (m)

In most cases of onshore pipelines, the coating and / or liner are thin and have a low elastic modulus relative to the pipe steel. The coating and / or liner provide a negligible stiffness contribution to the pipe wall. This contribution will be disregarded in the continuing development of the model below. Only the stiffness of the pipe wall will be included.

The deflection in the pipeline due to vertical load incurs a bending stress in the pipe wall. The maximum bending stress is given by [36]:

Equation 15: $$\sigma_{bend} = 4 \cdot E \cdot \left(\frac{\Delta y}{D}\right) \cdot \left(\frac{t}{D}\right)$$

where:

σ_{bend} bending stress in the pipe wall (Pa)

Equation 12 and Equation 15 above are used to calculate the bending stress in the pipe wall as a function of the pipeline dimensions and properties, and the loads acting on the pipeline due to soil weight and live loads. If it is assumed that the pipe will plastically collapse when the stress in the pipe wall exceeds the yield strength of the steel, it becomes possible to calculate the critical live load at the ground surface:

Equation 16: $$P_{cap} = \frac{2 \cdot \pi \cdot C^2}{3 \cdot F'} \cdot \left[\left(\frac{\sigma_{yield}}{4 \cdot E}\right) \cdot \left(\frac{D}{t}\right) \cdot \frac{(EI)_{eq} + 0.06 \cdot E' \cdot R^3}{L \cdot K \cdot R^3} - P_{soil}\right]$$

where:

P_{cap} load bearing capacity (N)

σ_{yield} yield strength of pipe steel (Pa)

In effect, the load bearing capacity is the critical live load at the ground surface that is predicted to cause plastic collapse of the pipe. If the critical load is zero, then the pipeline is predicted to collapse under the weight of soil alone. The above equation includes a simplification that the load is directly over the pipe. The use of yield strength is conservative. Another approach would be to use the flow stress (σ_{flow}).

Examination of the above equations reveals a non-intuitive result. The relationship between the critical collapse load and the wall thickness of the pipe is not a direct and simple one. Intuitively, the critical load should decrease with decreasing wall thickness of pipe. If a pipe wall were to corrode uniformly, one would expect the critical collapse load to decrease steadily. However, this is not the case. As the pipe wall becomes thinner, the compliance of the pipe wall increases, as shown in Equation 13 and Equation 14. For a given weight of soil and live load, the vertical deflection increases, as shown in Equation 12. This equation also shows an increase in vertical deflection with decreasing wall thickness. However, the decreasing wall thickness also leads to a decreasing bending stress acting in the pipe wall, as shown in Equation 15. The result is that the critical collapse load does not decrease steadily with decreasing wall thickness.

5.4 Elastic Collapse Model

An alternative approach to predicting the critical load necessary to cause collapse of the pipeline is to consider elastic collapse, also referred to as buckling. Buckling is illustrated schematically in Figure 22.

The critical buckling load is given by [36]:

Equation 17: $$P_{crit} = \frac{1}{FS}\sqrt{32 \cdot R_w \cdot B' \cdot E' \cdot \frac{(EI)_{eq}}{D^3}}$$

where:

- P_{crit} critical buckling load
- FS factor of safety (2.5 if C/D ≥ 2, 3.0 if C/D < 2)
- B' empirical coefficient of elastic support

Equation 18: $$B' = \frac{1}{1+4 \cdot exp\left[-0.065 \cdot \left(\frac{C}{D}\right)\right]}$$

If it is assumed that the pipe will elastically collapse when the stress in the pipe wall exceeds this critical value, it becomes possible to calculate the critical live load at the ground surface:

Equation 19: $$P_{cap} = \frac{2 \cdot \pi \cdot C^2}{3 \cdot F\prime} \cdot \left[\frac{1}{FS}\sqrt{32 \cdot R_w \cdot B' \cdot E' \cdot \frac{(EI)_{eq}}{D^3}} - P_{soil}\right]$$

In effect, the load bearing capacity is the critical live load at the ground surface that is predicted to cause elastic collapse of the pipe. If the critical load is zero, then the pipeline is predicted to collapse under the weight of soil alone. The above equation includes a simplification that the load is directly over the pipe.

In the case of elastic collapse of the pipeline, the critical load does decrease steadily with decreasing wall thickness in the pipe.

5.5 Combined Plastic and Elastic Collapse Models

Two simple structural models have been developed to predict the load bearing capacity of a buried pipeline of given outside diameter, wall thickness and depth of cover. The two models are based on (a) plastic collapse of the pipe due to the bending stress in the pipe wall exceeding the yield strength of the pipe steel, and (b) elastic collapse, or "buckling" of the pipe wall. Both models should be considered. The lower of the two critical load predictions will indicate the more likely failure mechanism. For many scenarios, the critical load will be governed by plastic collapse for the thicker walled pipe and elastic collapse as the pipe wall becomes thinner due to corrosion.

Consider a pipe of diameter 610 mm, wall thickness 9.5 mm, and yield strength 240 MPa. Assume a 1.2 m depth of cover, with soil density 1500 kg/m^3 and soil modulus of 10 MPa. These values represent a typical situation, and this will be considered as "base case" conditions to demonstrate the model and sensitivity of the various parameters.

Figure 23 is a plot of the load bearing capacity of the pipeline as a function of wall thickness. This represents the basic model. Note that the wall thickness on the X-axis is in reverse order. This is done so that the model can be later combined with the corrosion model, and the decreasing wall thickness is comparable to increasing corrosion time. The blue curve on the left side of the plot represents the load bearing capacity of the pipe, as determined assuming plastic collapse (yielding of pipe wall) and using Equation 16. The shape of the "U-curve" is the non-intuitive result discussed above. The load bearing capacity of the pipe does not necessarily decrease with decreasing wall thickness. The red curve on the right represents the load bearing capacity of the pipe, as determined assuming elastic collapse (buckling) and using Equation 19. In this case, the decrease in load bearing capacity with decreasing wall thickness does show an intuitive relation. The dashed line in the figure at 4.7 mm represents the critical thickness at which the likely failure mode transitions from plastic collapse to elastic collapse.

Figure 23 demonstrates that the load bearing capacity of the base case pipeline is nearly 60,000 kg. In principle, a 60-tonne weight, directly over the pipeline, would be necessary to cause collapse. The calculation is based on a point load, which is an unlikely scenario. In most realistic situations, any load over the pipe would be distributed over the ground surface, and this provides conservatism to the model. The load bearing capacity changes and decreases to zero as the wall thickness of the pipe decreases (moving right along the X-axis). However, the load bearing capacity remains substantial even for thin walled pipe. For example, if the pipe wall decreases to 2 mm, the load bearing capacity is still approximately 15-tonnes.

Figure 24 is a plot of the load bearing capacity as a function of wall thickness, and demonstrating the effect of varying diameter. The blue curve in the centre is equivalent to the combined critical blue and red curves of Figure 23, and representing the critical load for base case conditions, regardless of failure mechanism. The red and green curves represent the load bearing capacity of a larger diameter pipe (914 mm) and a smaller diameter pipe (323 mm), respectively. On the right side of the plot, the red curve representing the larger diameter pipe (914 mm) is lower than the other two curves, indicating that the larger diameter pipe has a lower load bearing capacity as the wall thickness decreases. This indicates that a larger diameter pipe is more likely to collapse than a smaller diameter pipe, all else being equal.

Figure 25 is a plot of the load bearing capacity as a function of wall thickness, and demonstrating the effect of varying depth of cover. Again, the blue curve in the centre represents the base case conditions. The red and green curves represent the load bearing capacity of a shallower (0.6 m) buried pipe and a deeper (1.8 m) buried pipe, respectively. The red curve representing the shallower (0.6 m) buried pipe is lower than the other two curves, indicating the shallower buried pipe has a lower load bearing capacity. This indicates that a shallower buried pipe is more likely to collapse than a deeper buried pipe, all else being equal.

Figure 26 is a plot of the load bearing capacity as a function of wall thickness, and demonstrating the effect of varying yield strength of the pipe. The blue curve represents base case conditions. The red and green curves represent two higher strength line pipe steels, of Grade 290 MPa and Grade 360 MPa, respectively. Grade 240 MPa was assumed the lowest likely grade of steel to be encountered, so two higher grades were selected for comparison. Unlike the previous two demonstrations, the yield strength of the pipe only affects the plastic collapse (left) side of the curve. Examination of Equation 19 indicates no relation between yield strength and critical load bearing capacity for elastic collapse. Therefore, the load bearing capacity of the pipe becomes independent of yield strength as the pipe wall decreases.

Figure 27 is a plot of the load bearing capacity as a function of wall thickness, and demonstrating the effect of varying soil modulus. The blue curve represents the base case. The red and green curves represent lower soil modulus (5 MPa) and higher soil modulus (20 MPa), respectively. A soil of modulus 5 MPa would likely be a finer grained soil with loose compaction. A soil of modulus 20 MPa would likely be a coarser grained soil with high compaction. The red curve representing the lower soil modulus (5 MPa) is lower than the other two curves, indicating the pipe buried in the soil with lower modulus has a lower load bearing capacity. This indicates that a pipe buried in lower modulus soil is more likely to collapse than a pipe buried in higher modulus soil, all else being equal.

The plots demonstrate the effect of varying diameter, depth of cover, yield strength and soil modulus. A larger diameter, shallower depth of cover, lower yield strength and low modulus all contribute to decreasing the load bearing capacity of the pipe. Consider the "extreme case" of all these factors varied from the base case, that is, consider a pipe of 914 mm diameter, 0.6 m depth of cover, 240 MPa yield strength and soil modulus 5 MPa. In addition, consider an initial wall thickness of 6.35 mm. This represents a very conservative combination of factors.

Figure 28 is plot of the load bearing capacity as a function of wall thickness for the "extreme case" conditions. Note that the load bearing capacity on the Y-axis has a range 10X less than the previous plots. The blue curve represents the extreme case. For the extreme case, the elastic collapse conditions are limiting for all wall thickness, so the left side of the curve does not show the characteristic plastic collapse "U-curve" observed in the previous plots. However, the load bearing capacity of the pipe remains substantial, even under these extreme conditions. This curve demonstrates that abandoned pipelines under "typical" conditions are not subject to imminent collapse.

It should also be noted that all of the above examples assume uniform wall loss. In effect, these curves represent bare pipe, with no corrosion protection coating, and with corrosion occurring over the entire surface of the pipe. This is very conservative but is not realistic.

Consider a pipeline with only 1% disbonded coating on the pipe surface. After several years of corrosion the pipe becomes perforated, and takes on the "Swiss cheese" characteristics. The pipeline becomes 99% nominal thickness pipe with 1% dispersed holes, areas of "zero" thickness. The above assumption that wall loss degrades uniformly over time becomes extremely conservative.

Consider the plastic collapse model. If 1% of the wall is lost due to corrosion, that is, the holes in the Swiss cheese, then the load bearing capacity decreases by only 1%. This assumes the holes are randomly dispersed around the circumference of the pipe. If the holes were clustered along the 3 and 9 o'clock orientations, where the stresses are highest, then the load bearing capacity would be further reduced. Consider if there were significant coating disbondment of 10%, the load bearing capacity would be decreased by only 10%. This rationale demonstrates that the approach used for the structural integrity modelling has significant inherent conservatism.

Figure 29 is a plot of load bearing capacity as a function of coating disbondment, for the base case conditions. This plot assumes nominal wall thickness for the majority of the pipe, but with corroded holes equal in area to the disbonded area. Note that the X-axis if plotted on a logarithmic scale. The plot demonstrates that the load bearing capacity of the pipe remains significant, if the disbonded area is up to ~10%. However, as the perforated area increases to 20% or 50% or more, this simple relationship likely breaks down, and it is not recommended that it be considered for significantly degraded pipe.

Consider the elastic collapse model. A simple correlation between perforated area and load bearing capacity is not valid. Elastic collapse equation derivations are very sensitive to geometry. It is not likely that the load bearing capacity scales linearly with perforated area. The calculations necessary to demonstrate this are considered beyond the scope of this modelling. This situation would only need to be considered if the assumption of bare pipe leads to problematic conclusions.

6.0 COMBINED CORROSION RATE AND STRUCTURAL INTEGRITY MODELLING

The above two sections describe the development of two models; a corrosion rate model and a structural integrity model. The corrosion rate model calculates the depth of corrosion as a function of time, or the remaining wall thickness as a function of time. The structural integrity model calculates the load bearing capacity as a function of wall thickness. There have been a few assumptions and modifications discussed during the development of the models to demonstrate how the models can be used. The objective of this section is to describe how the two models can be combined and used practically.

The corrosion rate model calculates the remaining wall thickness of pipe as a function of the corrosion rate and time using a simple relationship, expressed as Equation 4. The relationship between wall thickness and time is illustrated in Figure 19 for three different corrosion rates. The structural integrity model calculates the load bearing capacity of the pipe as a function of wall thickness, diameter, and material and soil properties. The relationships are expresses as Equation 16 and Equation 17 for plastic and elastic collapse respectively. The load bearing capacity is a strong function of wall thickness, as illustrated in Figure 23 through Figure 28. By combining the two models, it is possible to calculate the load bearing capacity as a function of time.

Figure 30 is a plot of the load bearing capacity as a function of time, for base case conditions (610 mm diameter, 9.5 mm wall thickness, 240 MPa yield strength, bare steel), for three different corrosion rates. The figure is essentially a combination of Figure 19 (wall thickness as a function of time for three different corrosion rates) and Figure 23 (load bearing capacity as a function of wall thickness). The plot demonstrates that, for the base case conditions, and under reasonable corrosion rates, structural integrity of the pipe will remain significant for hundreds or thousands of years. The shape of the curve is determined by the combination of the plastic and elastic collapse models and wall thickness loss over time as shown in Figure 23. Initially, load bearing capacity is limited by plastic collapse, but as the pipe wall corrodes, elastic collapse becomes the limiting failure mode, and the load bearing capacity of the pipe diminishes quickly with time. The spikes in each curve represent the change in failure mode.

Consider an example case in which a pipeline of 610 mm diameter, initial wall thickness of 9.5 mm and 240 MPa yield strength is abandoned in place and allow to freely corrode under typical soil conditions. Assume the soil is of average soil modulus, and the pipeline is buried at 1.2 m depth. These are considered "average" conditions. The model predicts that the pipeline will have sufficient structural integrity to support the weight of a personal truck (5,000 kg) for approximately 9,000 years before collapse.

Figure 31 is a plot of the load bearing capacity as a function of time, for the extreme case conditions, and assuming an upper bound corrosion rate (Soil #23). The figure is essentially Figure 28, but with a corrosion rate calculation included.

Consider an example case in which a pipeline of 914 mm diameter, initial wall thickness of 6.35mm and 240 MPa yield strength is abandoned in place and allow to freely corrode under extremely corrosive soil conditions. Assume the soil is of low soil modulus, and the pipeline is buried at 0.6 m depth. These are considered "extreme" conditions. The model predicts that the pipeline will have sufficient structural integrity to support the weight of a personal truck (5,000 kg) for approximately 90 years before collapse.

Note that both of the above plots assume a bare pipe and uniform wall loss.

It is of interest to this program to have a series of steps to determine the load bearing capacity of any pipeline at a given time:

1. **Compilation of data.** The calculations require the pipe diameter, wall thickness, material yield strength and modulus, depth of cover, modulus of soil reaction, and soil drainage (or estimate of relative corrosivity). The time used for calculations is also important. The time can be either the present, in which case the age of the pipeline may be used, or a time in the future.

2. **Determination of corrosion conditions**.

   a) If the pipe is uncoated, bare steel, then the soil drainage conditions should be estimated and a corrosion rate coefficient selected from Table 7. The table provides upper bounds for the soil types. A lower value can be selected at the modeler's discretion. The mass loss values are suggested for the structural integrity calculations, as they are indicative of overall damage to the pipe. Note that the assumption of bare steel is inherently conservative, and if results of the assessment are satisfactory, then further consideration of coating degradation is unnecessary.

   b) If the pipe is coated, then corrosion is only expected to occur at areas of disbonded coating. A corrosion coefficient may be selected, as above, but it is simpler to assume immediate through-wall penetration of the disbonded areas, and that the pipeline has the "Swiss cheese" character.

3. **Determination of wall thickness at the time of interest**.

   a) If the pipe is uncoated, bare steel, then the remaining wall thickness can be calculated using Equation 4 and the corrosion coefficient selected above.

   b) If the pipe is coated, it is deemed more suitable to assume nominal wall thickness for the majority of the pipe, and corrosion holes with an area comparable to the disbonded area.

4. **Determination of soils loads acting on the pipe**. Soils loads can be estimated using Equation 6 for basic conditions, Equation 7 for pipe below the water table, or Equation 9 for jacked pipe.

5. **Determination of critical loads**. There are two possibilities to consider:

   a) There are known live loads on the pipe, and the modeler is interested in determining whether the pipe is subject to collapse or not. In this case, the live loads can be calculated using Equation 10 for point loads, or Table 10 for standard distributed loads associated with vehicle traffic. The susceptibility to plastic collapse is determined using Equation 12 and Equation 15, and the calculated stress compared to the yield strength of the pipe material. The susceptibility to elastic collapse is determined using Equation 17, and the calculated critical load compared to the live loads acting on the pipe. Note that the remaining wall thickness is used for bare pipe and the nominal wall thickness is used for coated pipe. If coated, the resulting loads are scaled to account for the disbonded area.

   b) There are no specific loads, and the modeler is interested in determining the load bearing capacity of the pipe. In this case, the critical load bearing capacities are determined directly from Equation 16 and Equation 19, for plastic and elastic collapse, respectively. These equations were developed assuming an equivalent point load directly above the pipe. Again, the remaining wall thickness or nominal wall thickness of pipe is used for the calculation.

These steps provide a basic approach for determining the susceptibility of a pipeline to collapse under various conditions. It is based on several simplifications and assumptions, and these should be considered with the conclusion of the calculation.

Note that the methodology applied above could be used as the basis of a software program that would do the calculations automatically. This would allow analysts to consider the effect of various assumptions on the modelling results. Two examples are provided to demonstrate the use of the model:

6.1 Example 1

Consider a pipe of diameter 610 mm with wall thickness 6.35 mm, buried with a 1.2 m depth of cover, and bare steel grade 290 MPa. The soil is a coarse-grained soil with fines, with a 90% compaction, and density of 1400 kg/m^3*. The soil has fair drainage. It is of interest to determine the load bearing capacity of the pipe 75 years into the future.*

The pipe is bare steel, and therefore the entire pipe surface is subject to corrosion. Table 7 is consulted and k_{ml} = 0.10 mm/√yr is selected as an appropriate upper bound corrosion coefficient. The remaining wall thickness is calculated using Equation 4:

$$t = t_0 - k \cdot T^n = 6.35 - 0.10 \times 75^{0.5} = 5.5\, mm$$

A basic soil load will be assumed (no water table considerations or jacking). The soil load is calculated using Equation 6:

$$P_{soil} = \gamma_s \cdot C = 1400 \times 9.8 \times 1.2 = 16{,}464\, Pa$$

Note that the density of soil was reported as a mass, so the gravitational constant is included to convert to weight.

The load bearing capacity will be calculated considering both plastic and elastic collapse. For plastic collapse, use Equation 16:

$$P_{cap} = \frac{2 \cdot \pi \cdot C^2}{3 \cdot F'} \cdot \left[\left(\frac{\sigma_{yield}}{4 \cdot E} \right) \cdot \left(\frac{D}{t} \right) \cdot \frac{(EI)_{eq} + 0.06 \cdot E' \cdot R^3}{L \cdot K \cdot R^3} - P_{soil} \right]$$

This equation will be broken down for simplicity. The factor to convert live point loads at the surface to a distributed pressure on the top of the pipe is given by:

$$\frac{2 \cdot \pi \cdot C^2}{3 \cdot F'} = \frac{2 \times \pi \times 1.2^2}{3 \cdot 1} \approx 3$$

The term including the ratio of yield strength and modulus of steel is given by:

$$\left(\frac{\sigma_{yield}}{4 \cdot E} \right) = \left(\frac{290 \times 10^6}{4 \times 205 \times 10^9} \right) = 0.354 \times 10^{-3}$$

The equivalent stiffness of the pipe wall is given by:

$$(EI)_{eq} = E \times t^3/12 = 205 \times 10^9 \times (5.5 \times 10^{-3})^3/12 = 2842\, Pa \cdot m^3$$

Table 12 is consulted and 6.9 MPa is selected as an appropriate modulus of soil reaction. A lag factor of 1.5 and bedding constant of 0.1 will be assumed. The load bearing capacity against plastic collapse of the pipe is given by:

$$P_{cap} \approx 3 \times \left[0.354 \times 10^{-3} \times \left(\frac{610}{5.5}\right) \times \frac{2842 + 0.06 \times 6.9 \times 10^{6} \times 0.305^{3}}{1.5 \times 0.10 \times 0.305^{3}} - 16{,}464\right]$$

$$P_{cap} \approx 354{,}000\ N \rightarrow 36{,}100 kg \text{ (equivalent)}$$

The load bearing capacity of the pipe against plastic collapse is approximately 36-tonnes. For elastic collapse, use Equation 19:

$$P_{cap} = \frac{2 \cdot \pi \cdot C^{2}}{3 \cdot F'} \cdot \left[\frac{1}{FS}\sqrt{32 \cdot R_{w} \cdot B' \cdot E' \cdot \frac{(EI)_{eq}}{D^{3}}} - P_{soil}\right]$$

The water table is below the pipe, so the buoyancy factor is taken as unity. The empirical coefficient of elastic support is given by Equation 18:

$$B' = \frac{1}{1 + 4 \cdot exp\left[-0.065 \cdot \left(\frac{1.2}{0.610}\right)\right]} = 0.22$$

The load bearing capacity of the pipe against elastic collapse is given by:

$$P_{cap} \approx 3 \times \left[\frac{1}{3}\sqrt{32 \times 1 \times 0.22 \times 6.9 \times 10^{6} \times \frac{2842}{0.610^{3}}} - 16{,}464\right] \approx 730{,}500\ N \rightarrow 74{,}500\ kg$$

The load bearing capacity of the pipe against elastic collapse is approximately 74-tonnes.

The plastic collapse load of 36-tonnes is limiting.

6.2 Example 2

Consider a pipe of diameter 323 mm with wall thickness 9.5 mm, buried with a 0.9 m depth of cover. Assume 95% intact coating and steel grade 360 MPa. The soil is a fine-grained soil with 100% compaction, and density of 1600 kg/m^3. The soil has very poor drainage. It is of interest to determine the bending stress acting on the pipe wall if a 20-ton truck drives over the right of way.

The pipe is 95% coated, and therefore only 5% is subject to corrosion. For simplicity, assume that the disbonded area of the pipe has corroded through-wall, and the pipe has the Swiss cheese character. The nominal wall thickness of 9.5 mm will be used for calculations, and then later corrected for the disbonded area.

A basic soil load will be assumed (no water table considerations or jacking). The soil load is calculated using Equation 6:

$$P_{soil} = \gamma_s \cdot C = 1600 \times 9.8 \times 0.9 = 14{,}112\ Pa$$

The bending stress in the pipe wall is calculated from the deflection, which is calculated using the modified Iowa Equation 12:

$$\frac{\Delta y}{D} = \frac{L \cdot K \cdot \left(P_{soil} + P_{pipe}\right) \cdot R^3}{(EI)_{eq} + 0.061 \cdot E' \cdot R^3}$$

In this case, the live load acting on the pipe is due to vehicle traffic. Table 10 is consulted, and 29 kPa is selected as an appropriate effective load acting on the pipe due to a truck and 0.9 m of cover.

The equivalent stiffness of the pipe wall is given by:

$$(EI)_{eq} = E \times t^3/12 = 205 \times 10^9 \times (9.5 \times 10^{-3})^3/12 = 14{,}646\ Pa \cdot m^3$$

Table 12 is consulted and 10.4 MPa is selected as an appropriate modulus of soil reaction.

The vertical deflection in the pipe is given by:

$$\frac{\Delta y}{D} = \frac{1.5 \times 0.10 \times (14{,}112 + 29{,}000) \times 0.162^3}{14{,}646 + 0.061 \times 10.4 \times 10^6 \times 0.162^3} \approx 0.0016$$

The bending stress is given by Equation 15:

$$\sigma_{bend} = 4 \cdot E \cdot \left(\frac{\Delta y}{D}\right) \cdot \left(\frac{t}{D}\right) = 4 \times 205 \times 10^9 \times 0.0016 \times \left(\frac{9.5}{323}\right) \approx 38\ MPa$$

This calculation assumes full wall thickness and no corrosion. The stress must be scaled to account for the lost cross-sectional area of the pipe due to corrosion holes associated with disbonded coating. For 95 % intact coating and 5 % disbonded coating, the effective bending stress acting on the pipe wall is equal to (38 MPa / 95% intact =) 40 MPa.

7.0 SOIL COLLAPSE MODELLING

The above models have been developed to determine the times and loading conditions necessary for pipeline collapse. The result of the pipeline collapse is expected to be ground subsidence, as soil falls into the void of the empty pipe, and the local soil level lowers. It is of interest to the study to estimate the depth of ground subsidence in the event that a pipeline does collapse.

Consider the pipeline and soil geometry illustrated schematically in Figure 32. The pipeline is of diameter "D" and with depth of cover "C". Soil collapse typically occurs along 45° planes as the shear stresses are highest along these planes and so the soil slips along these planes. The 45° lines are projected from the centre of the pipeline to the ground surface to define a prism of soil subject to subsidence if the pipeline collapses. The area of the prism at the ground surface can be determined geometrically.

Assume the pipeline collapses and soil flows into the empty void of the pipeline. In order to simplify the calculations, it will be assumed the soil flows efficiently and fills the empty void. This is a conservative assumption. The volume of soil filling the pipeline can be calculated and used to estimate the depth of subsidence at the ground surface. Figure 33 is a schematic of the pipeline and soil geometry after pipeline collapse. The prism of soil subsides a depth "S", and this depth can be calculated geometrically.

The area of the pipeline filled by soil is given by:

Equation 20: $$A_{pipe} = \frac{\pi}{4} \cdot D^2$$

The area of the subsided soil above the pipeline is given by:

Equation 21: $$A_{soil} = (2 \cdot C + D) \cdot S - S^2$$

Note that areas of the pipeline and soil prism are used, but the actual geometry is a volume per unit length. Assuming these two volumes are equal:

Equation 22: $$S^2 - (2 \cdot C + D) \cdot S + \frac{\pi}{4} \cdot D^2 = 0$$

This equation can be solved using the quadratic formula to yield:

Equation 23: $$S = \frac{(2 \cdot C + D) - \sqrt{(2 \cdot C + D)^2 - \pi \cdot D^2}}{2}$$

However, a simplification of the geometry provides a more convenient estimate of the solution:

Equation 24: $$S \approx \frac{\pi}{4} \cdot \frac{D^2}{(2 \cdot C + D)}$$

This simplified solution is slightly (~10%) non-conservative for most pipe and soil geometries. It is recommended for typical pipeline conditions. The solution is less conservative for larger pipelines (> 1 m) with less depth of cover (< 1 m), and the solution provided by Equation 23 is recommended. Note that the assumption the soil flows freely and fills the pipeline void is inherently conservative.

Consider collapse of a pipeline of diameter 610 mm (ie. 0.610 m) with 1.2 m depth of cover. The depth of subsidence “S” is estimated as:

$$S \approx \frac{\pi}{4} \cdot \frac{0.610^2}{(2\times 1.2+0.610)} = 0.097 \text{ m} = 9.7 \text{ cm}$$

This represents a typical scenario.

Figure 34 is a simple plot of predict subsidence depth as a function of depth of cover and pipeline diameter. The data is based on Equation 23. For these previous two examples, provided in Section 6.0, the soil collapse model predicts depths of approximately 10 cm for the “average” case and 40 cm for the “extreme” case.

8.0 FURTHER DEVELOPMENTS

The models presented above need further development and refinement. Several options can be considered for further study. Field studies, laboratory studies, or further analyses could be performed to develop more precise models.

Excavation and examination of previously abandoned pipelines would provide valuable information that could be considered with respect to the assumptions made during the course of this study. Observations may confirm the assumptions used, or may provide guidance on how the current models should be modified for better predictions.

Laboratory experiments can also be considered. Bench top testing of soil with small-scale pipelines (tubing), or soil with simulated voids may lead to better understanding of the mechanical behavior of soil during pipeline deformation and soil collapse. Additional testing could be performed to evaluate corrosion rates under disbonded coatings and coating degradation rates in soils. Laboratory experiments have the advantage of providing accelerated testing, relative to the field studies that are expected to provide limited information for hundreds of years.

Further analyses, such as refined statistical modelling and finite element modelling, could provide predictions that complement the current models. Ideally, further studies and refinements to the models are complementary, and demonstrate self-consistent results that provide increased confidence in the current models.

9.0 SUMMARY

A literature review was performed to identify corrosion and structural integrity studies relevant to the development of predictive models to understand the degradation and collapse of abandoned pipelines. Several industry studies have been performed by other researchers that are relevant to this program. The data generated and the models developed by these studies have been reviewed.

Soils data generated by the NBS has been used to develop a corrosion rate model that is considered suitable for the pipeline abandonment program. The model is based on a parabolic rate law, and provides a reasonable upper bound estimate for corrosion rate calculations. The model can be modified easily to account for average or lower bound corrosion rate conditions. The methodology of the model has been discussed. Examples and plots have been provided to demonstrate the use and sensitivity of the model.

Established structural integrity and soil mechanics equations, developed primarily by the civil engineering industry and academia, have been combined to develop a structural model considered suitable for the pipeline abandonment program. The model is based on the assumption that soils loads and live loads acting above the pipe will lead to either plastic or elastic collapse of the pipeline at a critical level. The critical load acting on the pipe to cause this collapse is considered the load bearing capacity of the pipeline. The model can be modified to account for dry or wet soils, jacked installation of the pipeline, and personnel or vehicle traffic.

As shown by the analytical results of this study, the predicted time to collapse will vary depending on a number of variables, including (i) pipeline diameter, wall thickness and yield strength, (ii) soil type and soil properties, and (iii) pipeline depth of cover. Accordingly, analytical predictions have to be made on a case-specific basis using applicable pipeline and soil data.

The analysis suggests that a medium diameter pipeline situated in stable soil and at typical depth would support a personal truck for approximately 9,000 years before collapse. On the other hand, in a situation where a large diameter pipeline is buried at very shallow depth in extremely poor soil conditions, the pipeline may collapse under the weight of a truck in the time of approximately 100 years.

Note that the above examples assume the pipelines are not coated, and the bare steel surface is free to corrode. Generally, this is an inherently conservative assumption because there is no coating to retard the degradation of the pipe steel. If a coating were present, as is typically the case, the model would predict a higher load bearing capacity and / or a longer time to collapse. In some cases, corrosion rates can be faster at areas of coating disbondment than for a bare pipeline.

The corrosion rate and structural integrity models can be combined in a practical way to determine the load bearing capacity of the pipeline as a function of time. Instructions and examples have been provided in the use of the models. In addition, both bare steel pipelines and pipelines with coating and partial disbondment have been considered and discussed.

A simple geometric model has been developed to estimate the depth of soil subsidence in the event that a pipeline does collapse. The predicted depth of subsidence is highly variable depending on pipeline diameter, burial depth and soil type, but is generally expected to be less than 10 cm. At the very extreme, the predicted depth of subsidence could be up to about 40 cm for a large diameter pipeline buried at shallow depth in poor soil conditions. The area of disturbance would be much wider than the pipeline diameter due to the behavior of soil above the pipe.

The models developed within this study need further development and refinement.

10.0 LITERATURE

1. “Pipeline Abandonment: A Discussion Paper on Technical and Environmental Issues,” Pipeline Abandonment Steering Committee, November 1996.

2. “Pipeline Abandonment Assumptions: Technical and Environmental Considerations for Development of Pipeline Abandonment Strategies,” Terminal Negative Salvage Task Force of the Canadian Pipeline Association, April 2007.

3. “Pipeline Abandonment Assumptions – Technical and Environmental Considerations for Development of Pipeline Abandonment Strategies,” Canadian Energy Pipeline Association, April 2007.

4. “Land Matters Consultation Initiative Streams 1, 2 and 4 Final Report,” National Energy Board, May 2009.

5. DNV, “Pipeline Abandonment Scoping Study”, Report No. EP028844, November 2010.

6. “Uhlig’s Corrosion Handbook, Second Edition,” Editor R. Winston Revie, John Wiley & Sons Inc., 2000.

7. R.L. Starkey and K.M. Wight, “Anaerobic Corrosion of Iron in Soil,” American Gas Association Monograph, New York, 1945.

8. R. A. King, “A review of soil corrosiveness with particular reference to reinforced earths,” TRRL Supplementary Report 316, TRRL, Crowthorne, 1977.

9. “Handbook for Steel Drainage and Highway Construction Products, Fifth Edition,” American Iron and Steel Institute, 1994.

10. R. D Webster, “Pipeline Corrosion Evaluation,” Topical Report, Corrpro Canada Inc., 1995.

11. Albert Molinas and Amanullah Mommandi, “Development of New Corrosion / Abrasion guidelines for Selection of Culvert Pipe Materials,” Report No. CDOT-2009-11 Final Report, Colorado Department of Transportation, November 2009.

12. California Test 417, “Method of Testing Soils and Waters for Sulfate Content,” State of California – Business, Transportation and Housing Agency, Department of Transportation, March 2013.

13. California Test 422, "Method of Testing Soils and Waters for Chloride Content," State of California – Business, Transportation and Housing Agency, Department of Transportation, March 2013.

14. California Test 643, "Method for Estimating the Service Life of Steel Culverts," State of California – Business, Transportation and Housing Agency, Department of Transportation, November 1999.

15. California Test 643, "Method for Determining Field and Laboratory Resistivity and pH Measurements for Soil and Water," State of California – Business, Transportation and Housing Agency, Department of Transportation, June 2007.

16. "Corrosion Guidelines Version 2.0," California Department of Transportation, November 2012.

17. Underground Corrosion, Melvin Romanoff, NACE International, originally issued by National Bureau of Standards, April 1957.

18. Analysis of Pipeline Steel Corrosion Data from NBS (NIST) Studies Conducted between 1922-1940 and Relevance to Pipeline Management, Richard E. Ricker, NISTIR 7415, NIST May 2007.

19. Y. Katano, K. Miyata, H. Shimizu and T. Isogai, "Predictive Model for Pit Growth on Underground Pipelines," Corrosion Science Section, Corrosion, Vol. 59, No. 2, NACE International, February 2003.

20. James N. Mihell, David Coleman and Ryan Sporns, "Quantitative Evaluation of Indirect Inspection Reliability and Pipeline Reliability Based Statistical Methods," IPC2004-0057.

21. Andrew Francis, Marcus McCallum, Menno T. Van Os and Piet van Mastrigt, "A New Probabilistic Methodology for Undertaking External Corrosion Direct Assessment," IPC2006-10092.

22. Fraser King, Russell Given, Robert G. Worthingham and Greg van Boven, "Effect of Transitions in the Water Table and Soil Moisture Content on the Cathodic Protection of Buried Pipelines," IPC2006-10171.

23. L. Alfonso, F. Caleyo, J. M. Hallen, J. H. Espina-Hernandez and J. J. Escamilla-Davish, "Application of Extreme Value Statistics to the Prediction of Maximum Pit Depth in Non-Piggable Buried Pipelines," IPC2008-64351.

24. F. Caleyo, J. C. Velasquez, J. M. Hallen, J. E. Araujo and E. Perez-Baruch, “On the Probabilistic Distribution of External Pitting Corrosion in Buried Pipelines,” IPC 2008-64402.

25. R. E. Melchers, “Statistical Characterization of Pitting Corrosion – Part 2: Probabilistic Modelling for Maximum Pit Depth,” Corrosion Science Section, Corrosion, Vol. 61, No. 8, NACE International, August 2005.

26. J. Boussinesq, “Applications des Potentiels à l’Étude de l’Équilibre et Mouvement des Soildes Élastiques,” Gauthier-Villard, Paris 1885.

27. Highway Research Board, “The AASHTO Road Test Report 5 – Pavement Research,” HRB Special Report 61E, Washington, D.C., 1962.

28. G. A. Leonards and Robert Edward Stetkar, “Performance of Buried Flexible Conduits: Interim Report,” Joint Transportation Research Program, Joint Highway Research Project KHRP-78-24, Indiana Department of Transportation and Purdue University, 1978.

29. J. D. Hartley and J.M. Duncan, “E’ and its Variation with Depth,” ASCE Journal of Transportation Engineering, Volume 113, No 5, September 1987.

30. “Steel Pipe – A Guide for Design and Installation,” American Water Work Association Manual M11 Third Edition, 1989.

31. Ian D. Moore, Ernest T. Selig and Atef Haggag, “Elastic Buckling Strength of Buried Flexible Culverts,” Transportation Safety Research Record 1191, 1988.

32. P. Moser, “Buried Pipe Design,” McGraw Hill, 1990.

33. “The Civil Engineering Handbook,” Editor in Chief W. F. Chen, CRC Press, 1995.

34. R. Saunders, “Preliminary Geotechnical Assessment of Pipeline Subsidence Phenomena,” Topical Report, Geo-Engineering Ltd, 1995.

35. C. Basavaraju and William Saifung Sun, “Piping Handbook, Chapter B4 Stress Analysis of Piping Systems,” Editor Mohinder Nayyer, McGraw Hill, 1999.

36. American Lifelines Alliance, “Guidelines for the Design of Buried Steel Pipe,” American Society of Civil Engineers, July 2001.

37. “Concrete Pipe Design Manual, Chapter 4 Loads and Supporting Strengths,” American Concrete Pipe Association, 2001.

38. "Risk Informed Assessment of Degraded Buried Piping Systems in Nuclear Power Plants," NUREG/CR-6876, BNL-NUREG-7400-2005, Brookhaven National Laboratory, U.S. Nuclear Regulatory Commission, June 2005.

39. "Emerging Concepts for the Design of Pipeline Renewal Systems," Pipeline Infrastructure (PINS) Task Committee Report, American Society of Civil Engineers, June 2007.

40. David J. Warman, James D. Hart & Robert B. Francini, "Final Report: Development of a Pipeline Surface Loading Screening Process & Assessment of Surface Load Dispersing Methods," Canadian Energy Pipeline Association (CEPA), Final Report No. 05-44R1, October 16, 2009.

41. J. D. Palmer, Materials Performance 13(1), 41-46.

42. ASME B36.10M-2004, "Welded and Seamless Wrought Steel Pipe," American Society of Mechanical Engineers, 2004.

43. CSA Z245.1-07 "Steel Pipe" Canadian Standards Association, 2007.

44. CSA Z662-07 "Oil and Gas Pipeline Systems," Canadian Standards Association, 2007.

45. Fitness-for-Service, API 579-1 / ASME FFS-1, June 5, 2007.

Table 1. Classification of corrosivity based on aeration / drainage.[2]

Soil Type	Description of Soil	Aeration / Drainage	Water Table
I – Lightly Corrosive	1. Sands or sandy loams 2. Light textured silt loams 3. Porous loams or clay loams thoroughly oxidized to great depths	Good	Very low
II – Moderately Corrosive	1. Sandy loams 2. Silt loams 3. Clay loams	Fair	Low
III – Badly Corrosive	1. Clay loams 2. Clays	Poor	2 ft to 3 ft below surface
IV – Unusually Corrosive	1. Muck 2. Peat 3. Tidal marsh 4. Clays and inorganic soils	Very Poor	At surface, or extreme impermeability

Table 2. Classification of corrosivity based on resistivity.[3]

Resistivity Range (Ωcm)	Corrosivity
0 – 1,000	Very severe
1,001 – 2,000	Severe
2,001 – 5,000	Moderate
5,001 – 10,000	Mild
10,000+	Very Mild

2 Reference – recreated from Reference [11]
3 Reference [41].

Table 3. Typical resistivity values for soil and water[4].

Soil		Water	
Classification	**Resistivity (Ωcm)**	**Source**	**(Ωcm)**
Clay	750 – 2,000	Seawater	25
Loam	3,000 – 10,000	Brackish	2,000
Gravel	10,000 – 30,000	Drinking water	4,000+
Sand	30,000 – 50,000	Surface water	5,000+
Rock	50,000+	Distilled water	(infinite)

Table 4. Classification of soil corrosivity based on oxidation-reduction potential.[5]

Oxidation-Reduction Potential (mV Normal Hydrogen Electrode)	Degree of Corrosion
< 100	Severe
100 – 200	Moderate
200 – 400	Slight
> 400	Non-corrosive

[4] Reference [9].
[5] Reference [7].

Table 5. The forty-seven soil types used in the corrosion modelling [17].

Site	Soil Name	Location	Type	Internal Drainage
1	Allis silt loam	OH	silt loam	Poor
2	Bell clay	TX	clay	Poor
3	Cecil clay loam	GA	clay loam	Good
4	Chester loam	PA	loam	Fair
5	Dublin clay adobe	CA	clay	Poor
6	Everette gravelly sand loam	WA	sand loam	Good
7	Maddox silt loam	OH	silt loam	Fair
8	Fargo clay loam	ND	clay loam	Poor
9	Genessee silt loam	OH	silt loam	Poor
10	Gloucester sandy loam	MA	sand loam	Fair
11	Hagerstown loam	MD	loam	Good
12	Hanford fine sandy loam	CA	sand loam	Fair
13	Hanford very fine sandy loam	CA	sand loam	Fair
14	Hempsted silt loam	MN	silt loam	Fair
15	Houston black clay	TX	clay	Poor
16	Kalmia fine sandy loam	AL	sand loam	Fair
17	Keyport loam	VA	loam	Poor
18	Knox silt loam	NE	silt loam	Good
19	Lindley silt loam	IA	silt loam	Good
20	Mahoning silt loam	OH	silt loam	Poor
21	Marshall silt loam	MO	silt loam	Fair
22	Memphis silt loam	TN	silt loam	Good
23	Merced silt loam	CA	silt loam	Fair
24	Merrimac gravelly sandy loam	MA	sand loam	Good
25	Miami clay loam	WI	clay loam	Fair
26	Miami silt loam	OH	silt loam	Good
27	Miller clay	LA	clay	Poor
28	Montezuma clay adobe	CA	clay	Poor
29	Muck	LA	muck	Very poor

Site	Soil Name	Location	Type	Internal Drainage
30	Muscatine silt loam	IA	silt loam	Poor
31	Norfolk fine sand	FL	sand loam	Good
32	Ontario loam	NY	loam	Good
33	Peat	WI	peat	Very poor
34	Penn silt loam	PA	silt loam	Fair
35	Romona loam	CA	loam	Good
36	Ruston sandy loam	MS	sand loam	Good
37	St. John's fine sand	FL	sand	Poor
38	Sassafras gravelly sandy loam	NJ	sand loam	Good
39	Sassafras silt loam	DE	silt loam	Fair
40	Sharkey clay	LA	clay	Poor
41	Summit silt loam	MO	silt loam	Fair
42	Susquehanna clay	MS	clay	Poor
43	Tidal marsh	NJ	marsh	Very poor
44	Wabash silt loam	NE	silt loam	Good
45	Unidentified alkali soil	WY	soil	Poor
46	Unidentified sandy loam	CO	sand loam	Good
47	Unidentified silt loam	UT	silt loam	Poor

Table 6. Properties of the forty-seven soil types used as the basis of the corrosion modelling[17].

Site	pH	Resistivity [6] (Ω-m)	Total Acidity (mol/kg)	Na+K as [Na+] (mol/kg)	$[Ca^{2+}]$ (mol/kg)	$[Mg^{2+}]$ (mol/kg)	$[CO_3^{2-}]$ (mol/kg)	$[HCO_3^-]$ (mol/kg)	$[Cl^-]$ (mol/kg)	$[SO_4^{2-}]$ (mol/kg)
1	7.0	12.2	0.110	0.007	0.003	0.004	0.000	0.001	0.001	0.008
2	7.3	6.8	0.035	0.003	0.011	0.001	0.000	0.012	0.000	0.002
3	5.2	300	0.120							
4	5.6	66.7	0.076							
5	7.0	13.5	0.065	0.009	0.005		0.000	0.007	0.000	0.003
6	5.9	451	0.130							0.000
7	4.4	21.2	0.300							0.000
8	7.6	3.5		0.014	0.017	0.026	0.000	0.007	0.000	0.044
9	6.8	28.2	0.072							
10	6.6	74.6	0.036							
11	5.3	110	0.110						0.000	0.000
12	7.1	31.9	0.025	0.004	0.005	0.002	0.000	0.004	0.000	0.001
13	9.5	2.9		0.062	0.001	0.001	0.000	0.011	0.016	0.038
14	6.2	35.2	0.056							
15	7.5	4.9	0.050	0.022	0.009	0.002	0.000	0.020	0.001	0.007
16	4.4	82.9	0.120							
17	4.5	59.8	0.190							
18	7.3	14.1	0.014	0.003	0.006	0.002	0.000	0.009	0.000	0.003
19	4.6	19.7	0.110	0.004	0.003	0.004	0.000	0.002	0.000	0.005

6 Note that resistivity is listed in units of (Ω-m), whereas previous tables in the report listed in units of (Ω-cm)

Site	pH	Resistivity [6] (Ω-m)	Total Acidity (mol/kg)	Na+K as [Na+] (mol/kg)	[Ca^{2+}] (mol/kg)	[Mg^{2+}] (mol/kg)	[CO_3^{2-}] (mol/kg)	[HCO_3^-] (mol/kg)	[Cl^-] (mol/kg)	[SO_4^{2-}] (mol/kg)
20	7.5	28.7	0.015	0.003	0.005	0.002	0.000	0.005	0.000	0.002
21	6.2	23.7	0.095							
22	4.9	51.5	0.097							
23	9.4	2.8		0.084	0.004	0.002	0.000	0.019	0.011	0.056
24	4.5	114	0.130							
25	7.2	17.8	0.047	0.002	0.007	0.004	0.000	0.010	0.000	0.001
26	7.3	29.8	0.026	0.003	0.005	0.003	0.000	0.007	0.000	0.001
27	6.6	5.7	0.037	0.005	0.019	0.011	0.000	0.020	0.001	0.015
28	6.8	4.1		0.015	0.001	0.002	0.000	0.001	0.010	0.009
29	4.2	12.7	0.280	0.022	0.019	0.016	0.000	0.000	0.017	0.023
30	7.0	13	0.026	0.003	0.007	0.004	0.000	0.007	0.001	0.002
31	4.7	205	0.018							
32	7.3	57	0.005	0.002	0.007	0.001	0.000	0.007	0.000	0.004
33	6.8	8	0.360	0.015	0.073	0.041	0.000		0.023	0.021
34	6.7	49	0.070							
35	7.3	20.6	0.057	0.007	0.007	0.005	0.000	0.011	0.001	0.004
36	4.5	112	0.046							
37	3.8	112	0.150							
38	4.5	386	0.017							
39	5.6	74.4	0.066							
40	6.0	9.7	0.094	0.006	0.006	0.004	0.000	0.009	0.001	0.003

Site	pH	Resistivity [6] (Ω-m)	Total Acidity (mol/kg)	Na+K as [Na+] (mol/kg)	[Ca^{2+}] (mol/kg)	[Mg^{2+}] (mol/kg)	[CO_3^{2-}] (mol/kg)	[HCO_3^-] (mol/kg)	[Cl^-] (mol/kg)	[SO_4^{2-}] (mol/kg)
41	5.5	13.2	0.110	0.003	0.005	0.004	0.000	0.008	0.000	0.005
42	4.7	137	0.280							
43	3.1	0.6	0.370	0.450	0.052	0.095	0.000	0.000	0.430	0.370
44	5.8	10	0.088	0.011	0.011	0.007	0.000	0.020	0.008	0.004
45	7.4	2.6		0.082	0.037	0.007	0.000	0.002	0.002	0.120
46	7.0	15								
47	7.6	17.7	0.030	0.007	0.007	0.004	0.000	0.009	0.001	0.005

Table 7. Upper bound curve fit data for the NBS soils data.

Soil Type (Internal Drainage)	Coefficient for Mass Loss Data (k_{ml}) (mm/√yr)	Coefficient for Penetration Data (k_p) (mm/√yr)	Exponents for All Data (n)	Penetration Ratio
Good	0.05	0.75	0.5	15
Fair	0.10	1.0	0.5	10
Poor	0.15	1.0	0.5	6.7
Very Poor	0.20	1.0	0.5	5
All data	0.25	1.0	0.5	4

Table 8. Impact factors to be applied to live loads.[7]

Installation Surface Condition					
Height of Cover (ft)	**Height of Cover (m)**	**Highways**	**Railways**	**Runways**	**Taxiways, aprons, hardstands, run-up pads**
0 – 1	0 – 0.3	1.50	1.75	1.00	1.50
1 – 2	0.3 – 0.6	1.35	1.50	1.00	1.35
2 – 3	0.6 – 0.9	1.15	1.50	1.00	1.35
Over 3	Over 0.9	1.00	1.35	1.00	1.15

[7] Table recreated from Reference [36] Table 4.1-2, with the second column appended.

Table 9. Live loads transferred to pipe (psi).[8]

LIVE LOADS TRANSFERRED TO PIPE (psi)			
Height of Cover (ft)	**Highway H20** [9]	**Railway E80** [10]	**Airport** [11]
1	12.5	–	–
2	5.56	26.39	13.14
3	4.17	23.61	12.28
4	2.78	18.4	11.27
5	1.74	16.67	10.09
6	1.39	15.63	8.79
7	1.22	12.15	7.85
8	0.69	11.11	6.93
10	–	7.64	6.09
12	–	5.56	4.76
14	–	4.17	3.06
16	–	3.47	2.29
18	–	2.78	1.91
20	–	2.08	1.53
22	–	1.91	1.14
24	–	1.74	1.05
26	–	1.39	–
28	–	1.04	–
30	–	0.69	–
35	–	–	–
40	–	–	–

8 Table recreated from Reference [36] Table 4.1-1.
9 Simulates a 20-ton truck traffic load, with impact.
10 Simulates an 80,000 lb/ft railway load, with impact.
11 Simulates 180,000 lb dual tandem gear assemble, 26-inch spacing between tires and 66 inch centre-to-centre spacing between fore and aft tires under a rigid pavement 12 inches thick, with impact.

Table 10. Live loads transferred to pipe (kPa).[12]

LIVE LOADS TRANSFERRED TO PIPE (kPa)				ADDENDUM	
Height of Cover (m)	Highway H20 [13]	Railway E80 [14]	Airport [15]	Personal Truck [16]	Person [17]
0.3	86	–	–	21.6	5.0
0.6	38	182	91	9.6	1.3
0.9	29	163	85	7.2	0.6
1.2	19	127	78	4.8	0.3
1.5	12	115	70	3.0	0.2
1.8	10	108	61	2.4	0.1
2.1	8	84	54	2.1	0.1
2.4	5	77	48	1.2	0.1
3.0	–	53	42	–	–
3.7	–	38	33	–	–
4.3	–	29	21	–	–
4.9	–	24	16	–	–
5.5	–	19	13	–	–
6.1	–	14	11	–	–
6.7	–	13	8	–	–
7.3	–	12	7	–	–
7.9	–	10	–	–	–
8.5	–	7	–	–	–
9.1	–	5	–	–	–
10.7	–	–	–	–	–
12.2	–	–	–	–	–

12 Table recreated from Table 9 above, and with unit conversion to metric and two right side columns appended.
13 Simulates a 20-tonne truck traffic load, with impact.
14 Simulates an 11 tonne / m railway load, with impact.
15 Simulates 82 tonne dual tandem gear assembly, 0.66 m spacing between tires and 1.68 m centre-to-centre spacing between fore and aft tires under a rigid pavement 30 cm inches thick, with impact.
16 Simulates a 5 tonne personal truck load, with impact
17 Assumes 100 kg person, no impact

Table 11. Design values for soil modulus of reaction (psi).[18]

Type of Soil	Depth of Cover (ft)	Standard AASHTO Relative Compaction			
		85%	90%	95%	100%
Fine-grained soils with less than 25 % sand content (CL,ML,CL-ML)	0-5	500	700	1,000	1,500
	5-10	600	100	1,400	2,000
	10-15	700	1,200	1,600	2,300
	15-20	800	1,300	1,800	2,600
Coarse-grained soils with fines (SM, SC)	0-5	600	1,000	1,200	1,900
	5-10	900	1,400	1,800	2,700
	10-15	100	1,500	2,100	3,200
	15-20	1,100	1,600	2,400	3,700
Coarse-grained soils with little or no fines (SP, SW, GP, GW)	0-5	700	1,000	1,600	2,500
	5-10	1,000	1,500	2,200	3,300
	10-15	1,050	1,600	2,400	3,600
	15-20	1,100	1,700	2,500	3,800

18 Table recreated from [40, Table 2-3, 29].

Table 12. Design values for soil modulus of reaction (MPa).[19]

Type of Soil	Depth of Cover (m)	Standard AASHTO Relative Compaction			
		85%	90%	95%	100%
Fine-grained soils with less than 25 % sand content (CL,ML,CL-ML)	0-1.5	3.5	4.8	6.9	10.4
	1.5-3.0	4.1	0.7	9.7	13.8
	3.0-4.5	4.8	8.3	11.0	15.9
	4.5-6.0	5.5	9.0	12.4	18.0
Coarse-grained soils with fines (SM, SC)	0-1.5	4.1	6.9	8.3	13.1
	1.5-3.0	6.2	9.7	12.4	18.6
	3.0-4.5	0.7	10.4	14.5	22.1
	4.5-6.0	7.6	11.0	16.6	25.5
Coarse-grained soils with little or no fines (SP, SW, GP, GW)	0-1.5	4.8	6.9	11.0	17.3
	1.5-3.0	6.9	10.4	15.2	22.8
	3.0-4.5	7.2	11.0	16.6	24.9
	4.5-6.0	7.6	11.7	17.3	26.2

19 Table recreated from Table 12 above and with unit conversion to metric.

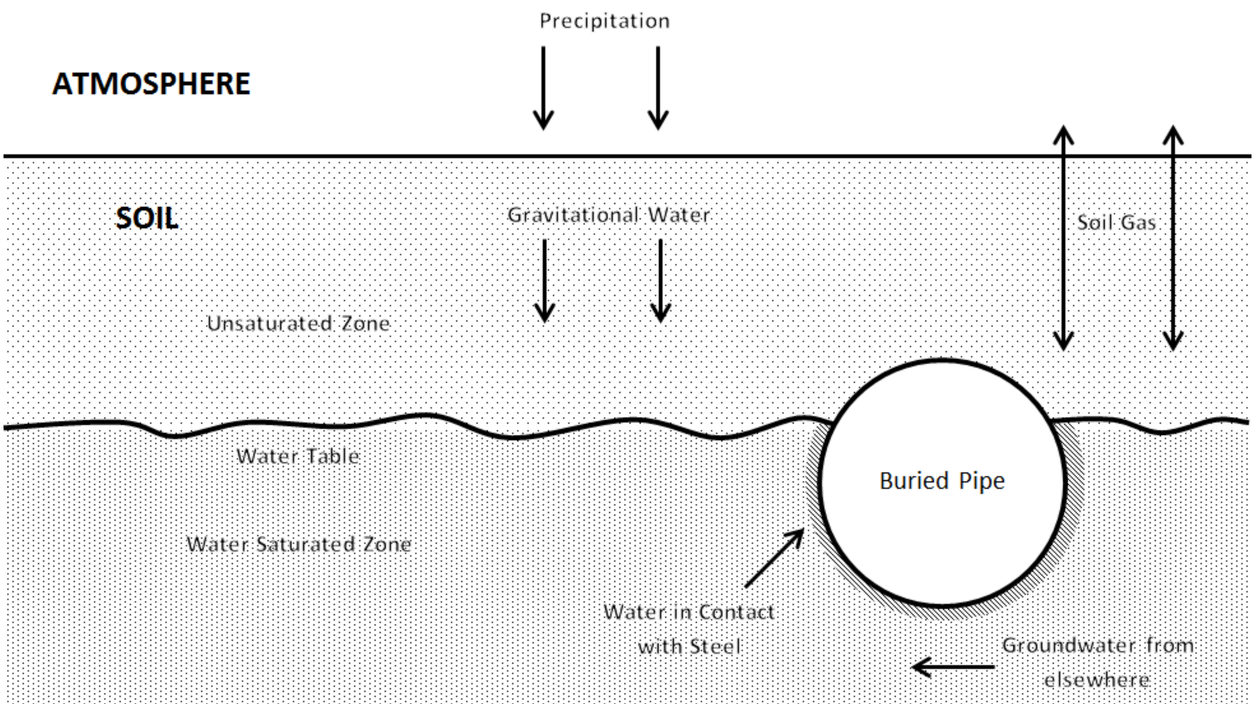

Figure 1. A schematic of a pipeline buried in soil and illustrating the local environment.

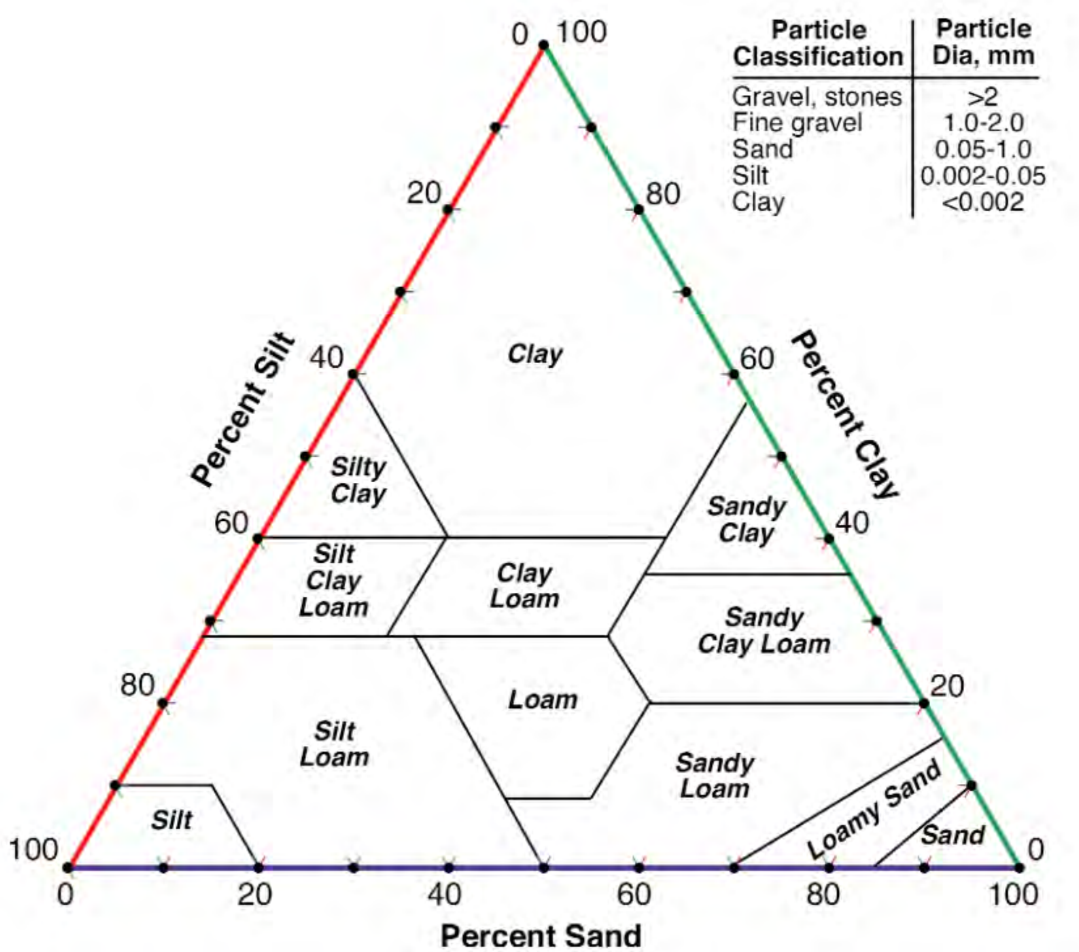

Figure 2. A ternary diagram describing soils types by characteristic particle sizes [18].

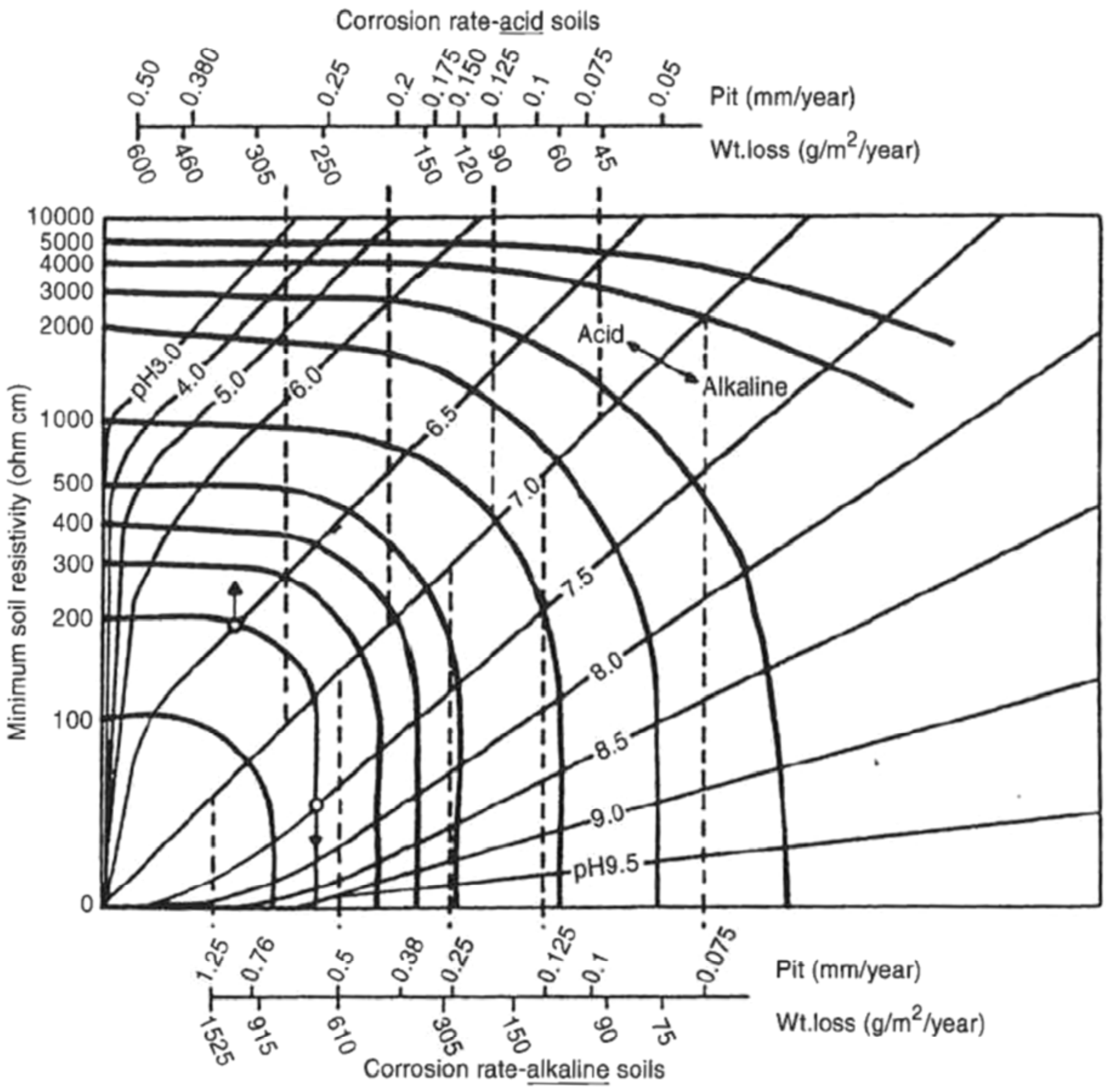

Figure 3. A nomogram relating soil resistivity, pH and corrosion rate for steel pipe in soil [8].

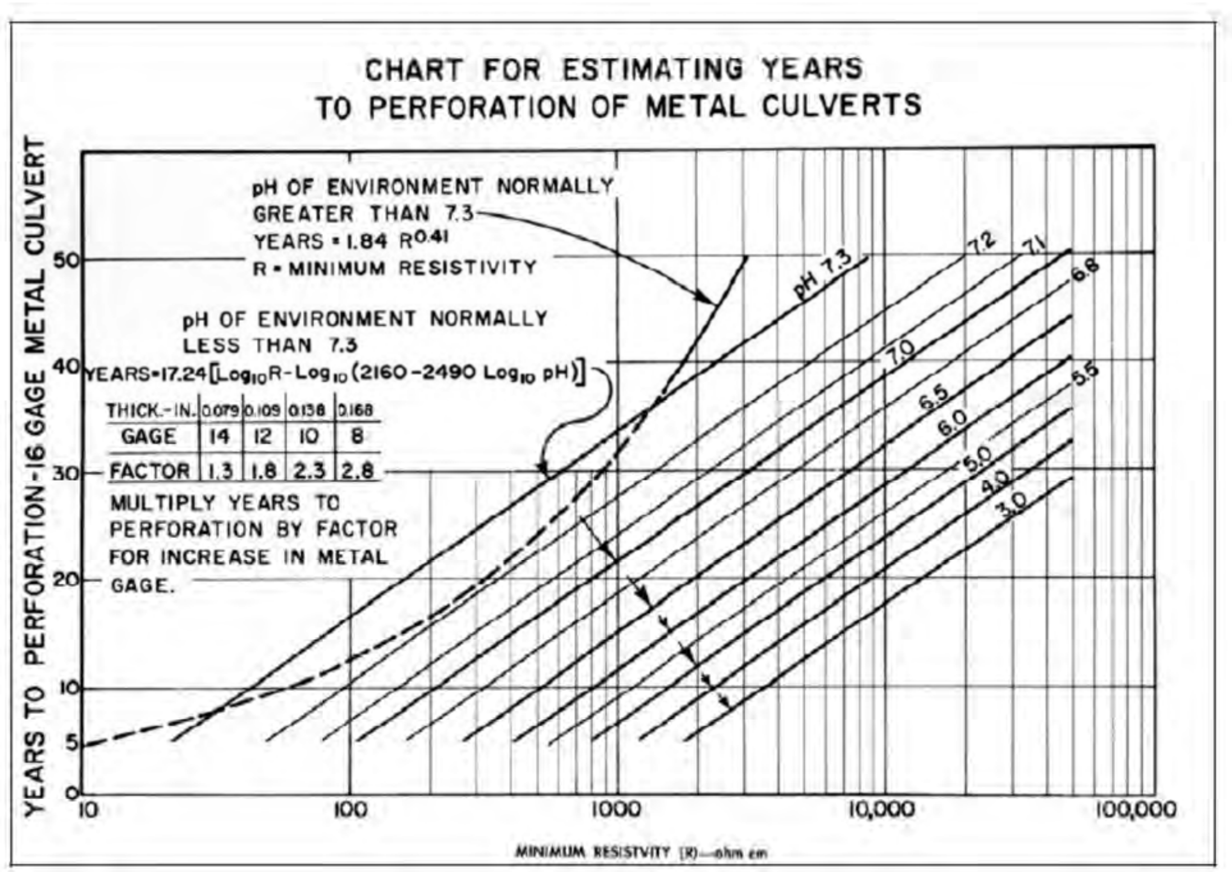

Figure 4. The California DOT method for determining service life for steel pipelines [11].

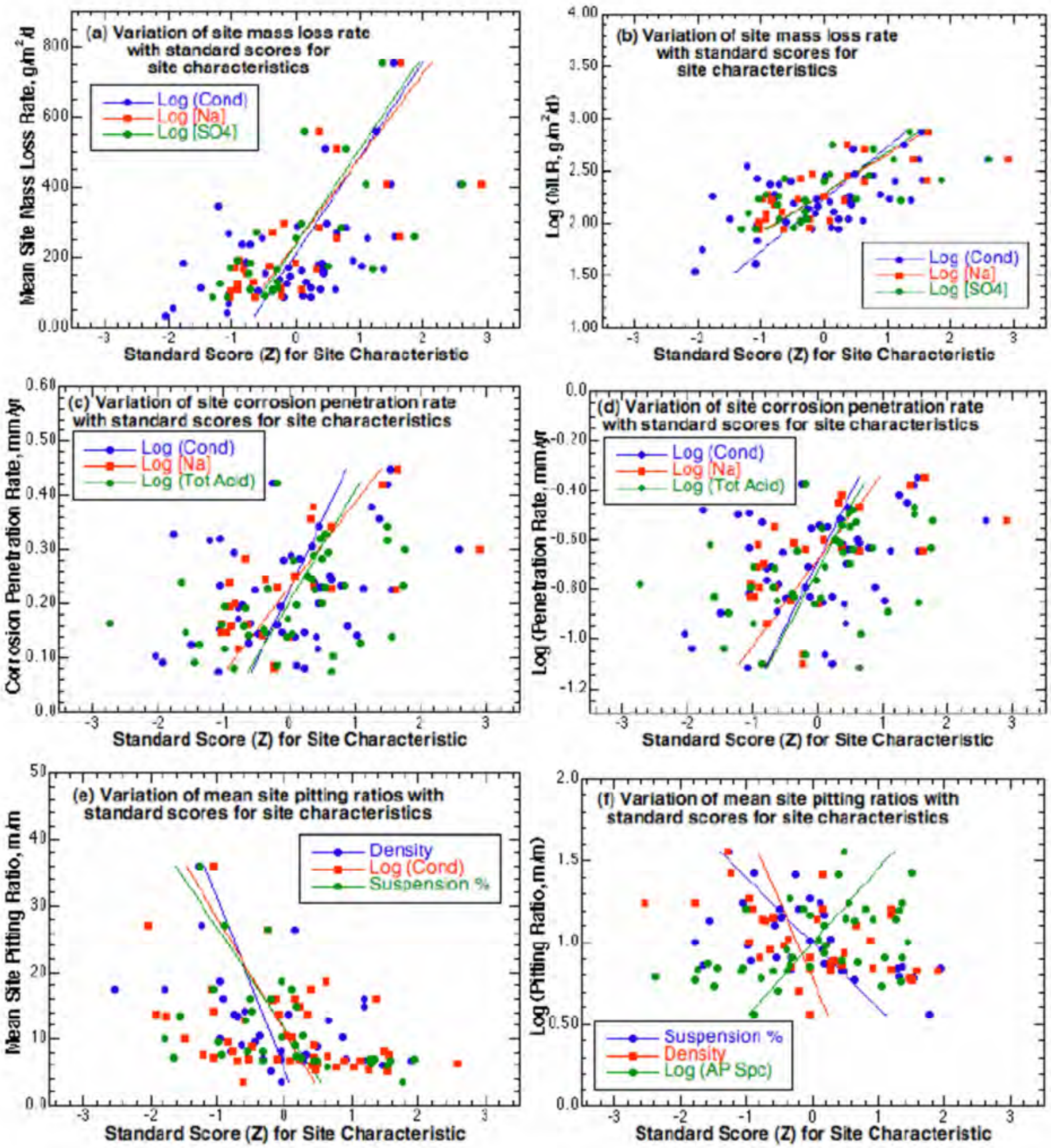

Figure 5. A selection of plots prepared during the statistical analysis of NBS soils corrosion data [18].

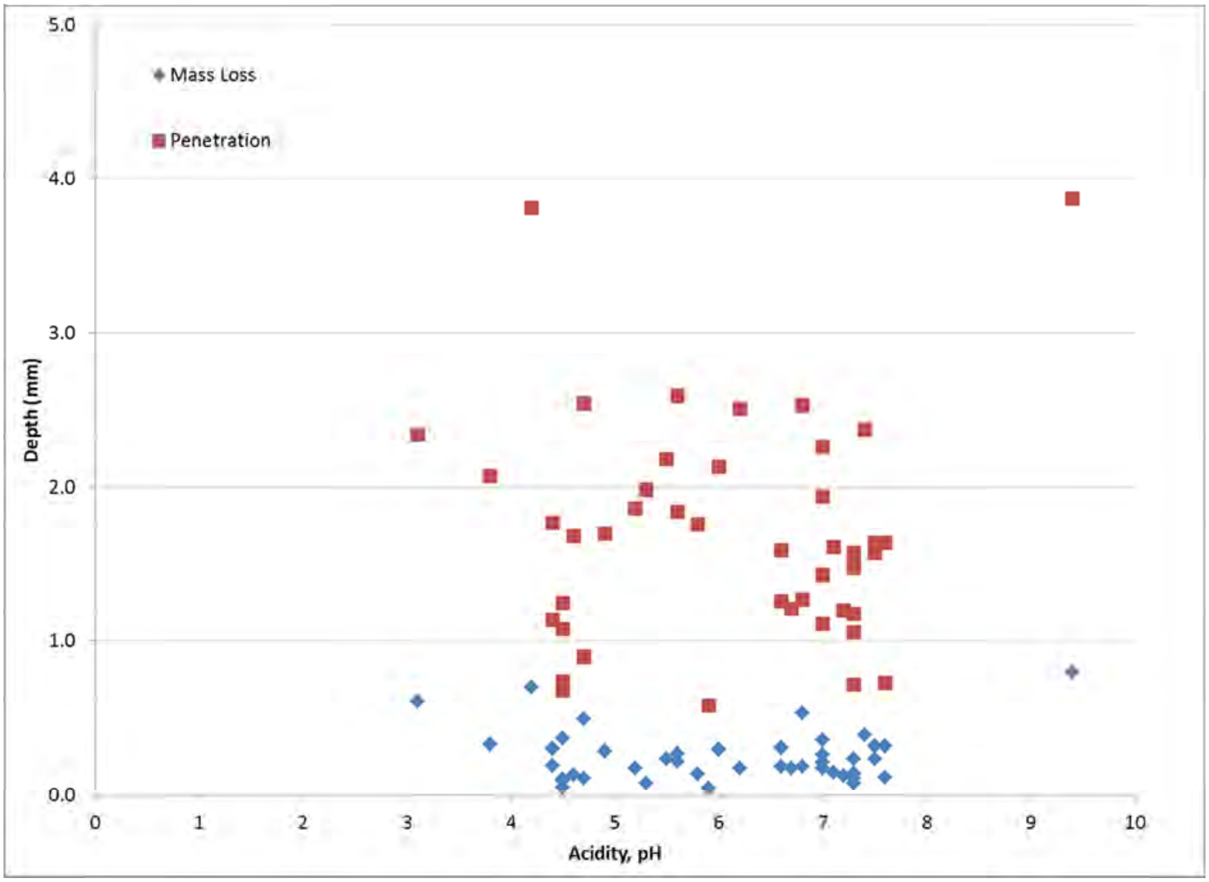

Figure 6. Plot of NBS corrosion depth data after ~12 years exposure as a function of acidity.

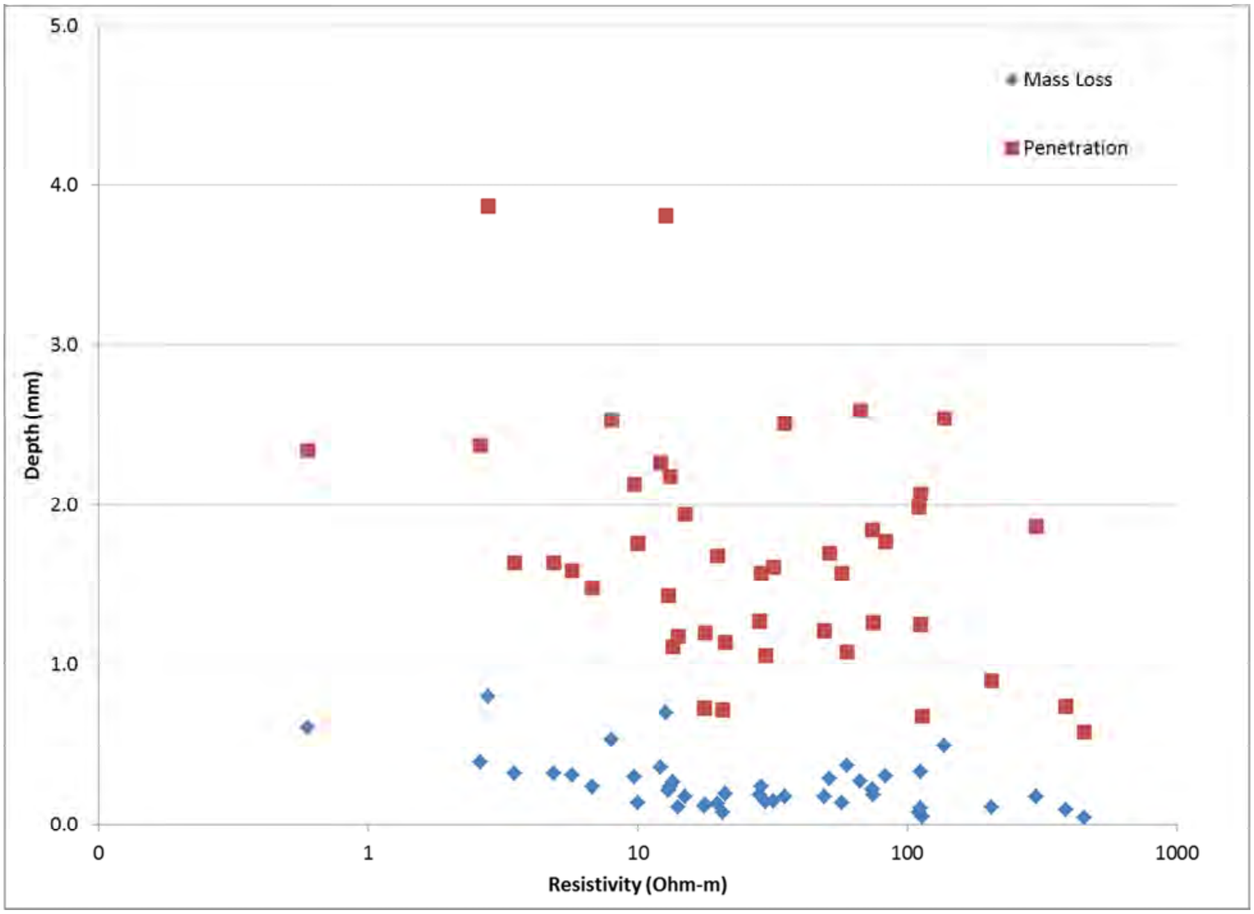

Figure 7. Plot of NBS corrosion depth data after ~12 years exposure as a function of resistivity.

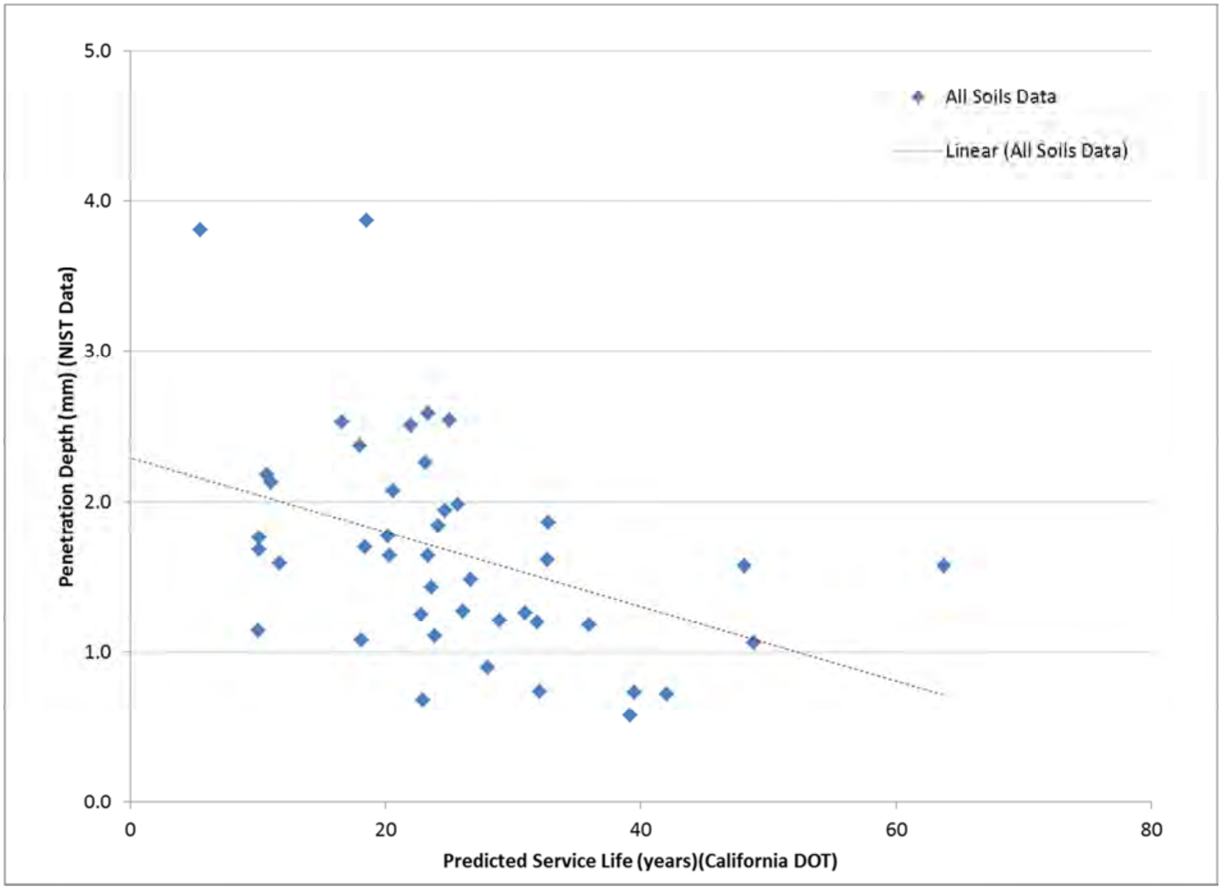

Figure 8. Plot of NBS penetration depth data at ~12 years as a function of the California DOT model prediction.

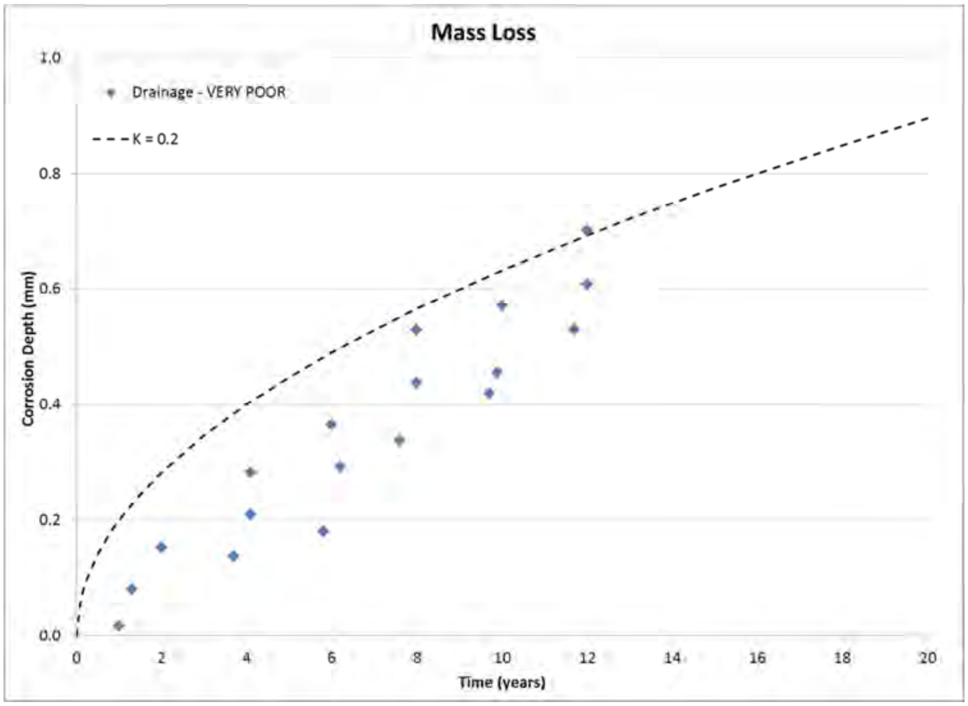

Figure 9. Plot of corrosion depth based on mass loss as a function of time for the soils with VERY POOR internal drainage.

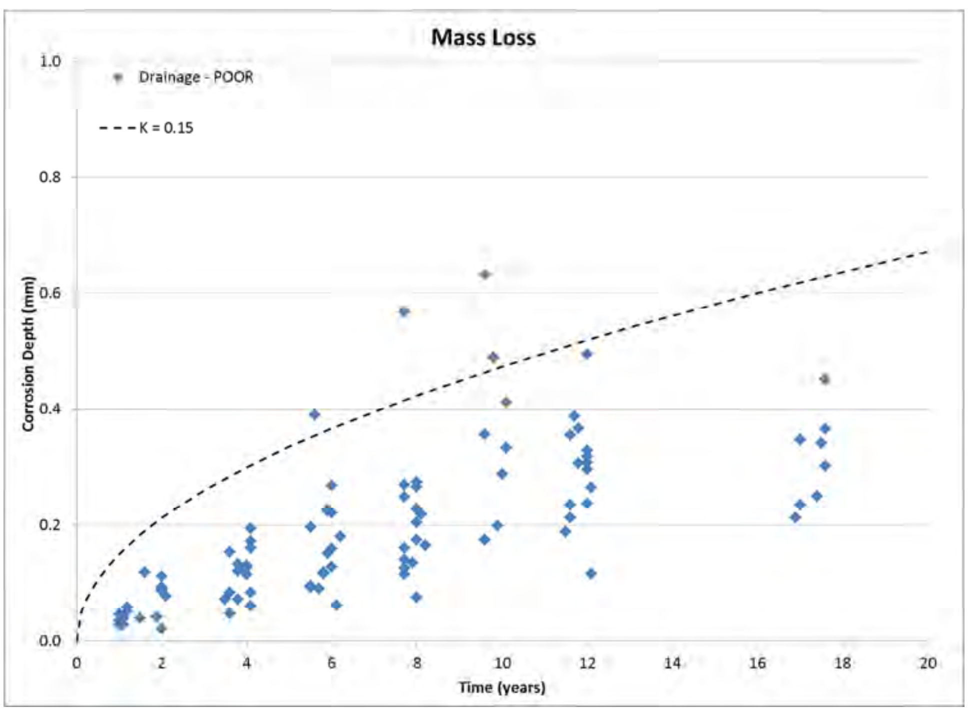

Figure 10. Plot of corrosion depth based on mass loss data as a function of time for the soils with POOR internal drainage.

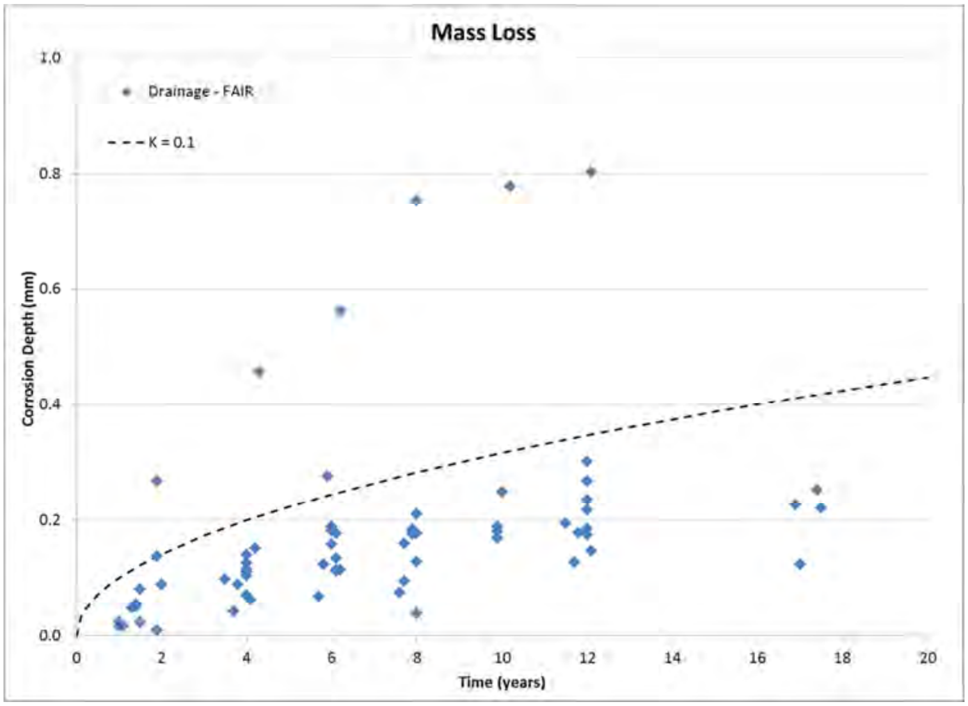

Figure 11. Plot of corrosion depth based on mass loss data as a function of time for the soils with FAIR internal drainage.

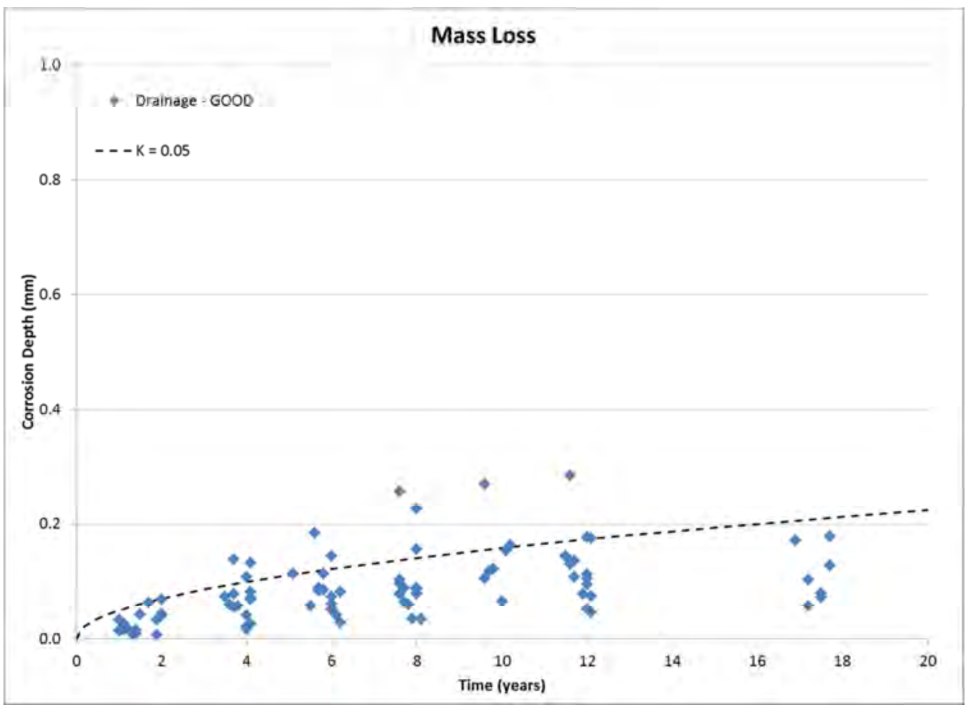

Figure 12. Plot of corrosion depth based on mass loss data as a function of time for the soils with GOOD internal drainage.

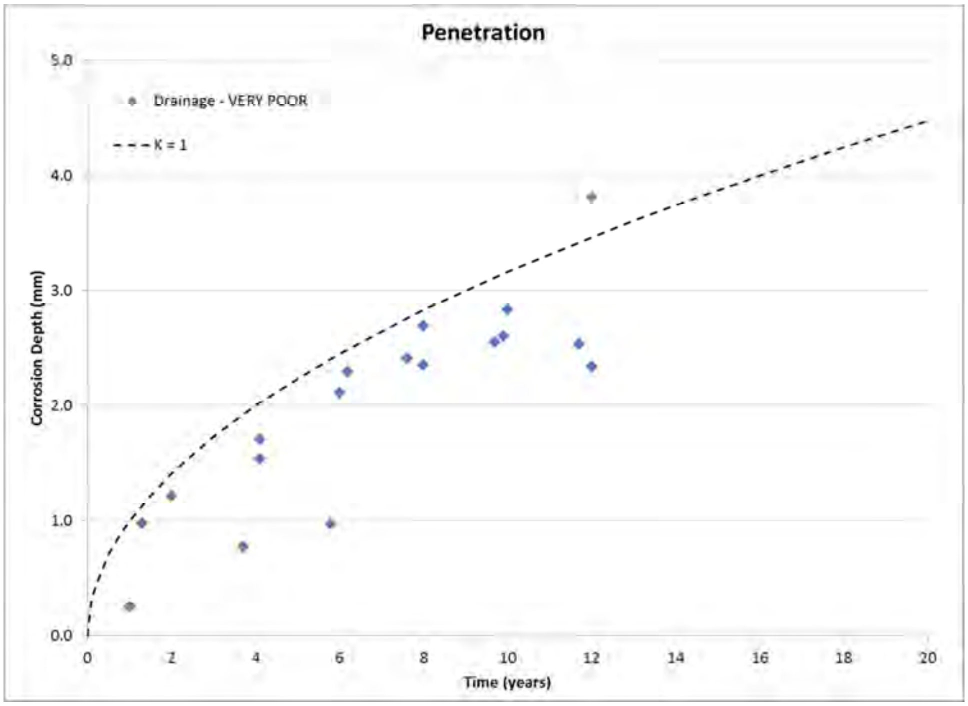

Figure 13. Plot of penetration depth data as a function of time for the soils with VERY POOR internal drainage.

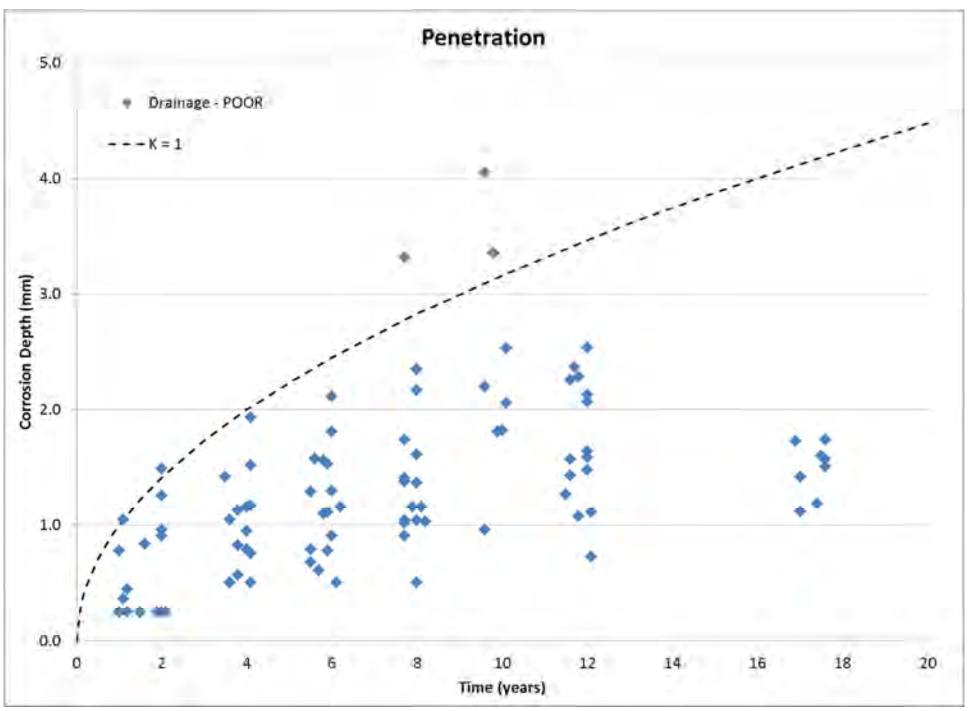

Figure 14. Plot of penetration depth data as a function of time for the soils with POOR internal drainage.

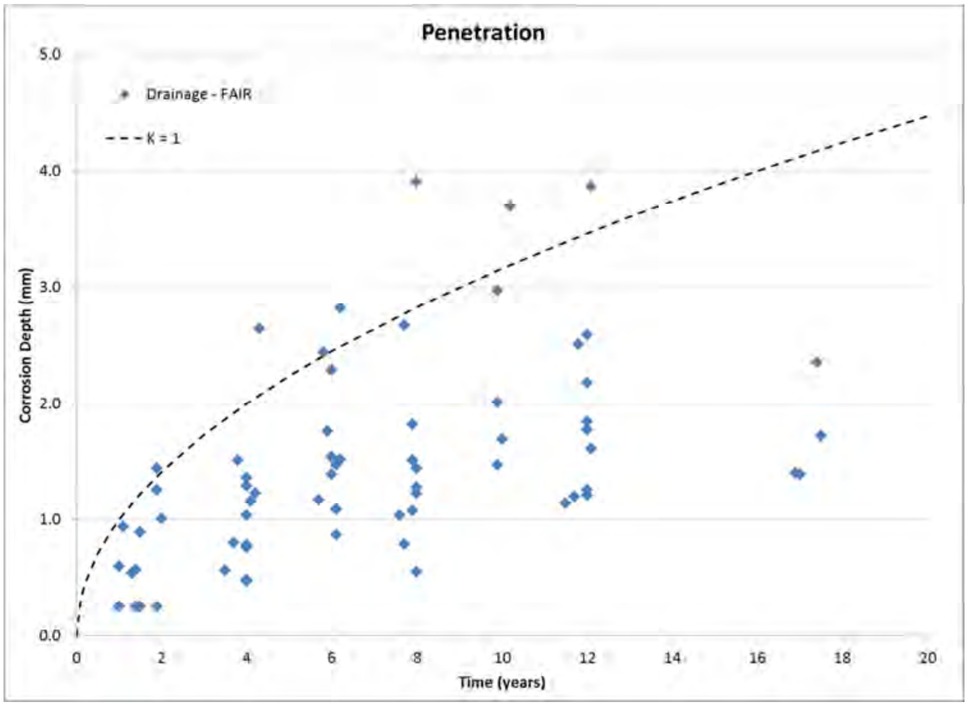

Figure 15. Plot of penetration depth data as a function of time for the soils with FAIR internal drainage.

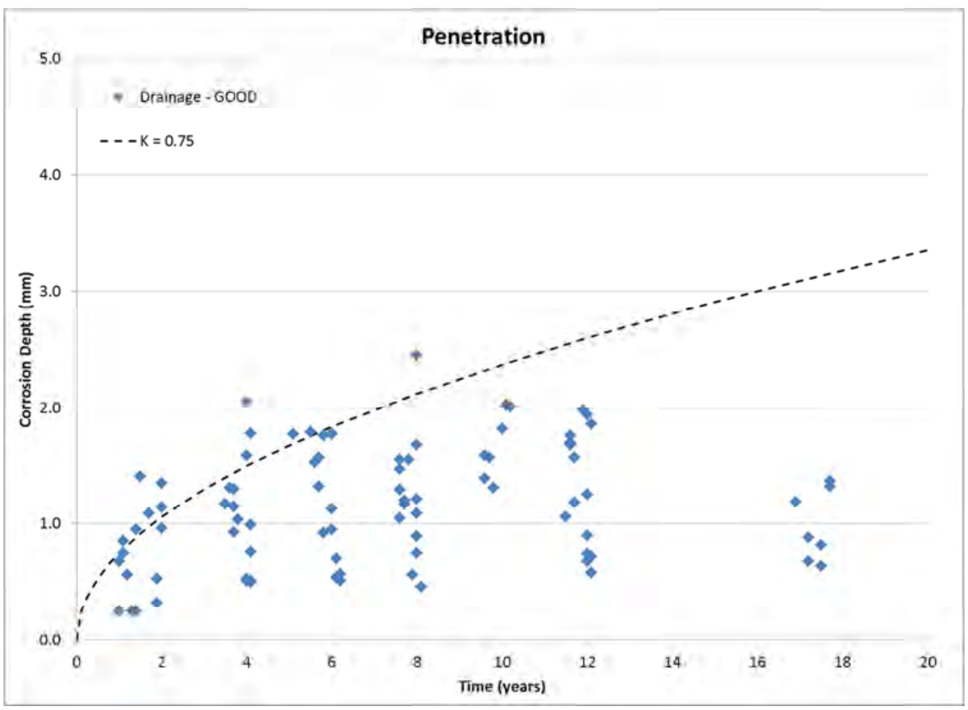

Figure 16. Plot of penetration depth data as a function of time for the soils with GOOD internal drainage.

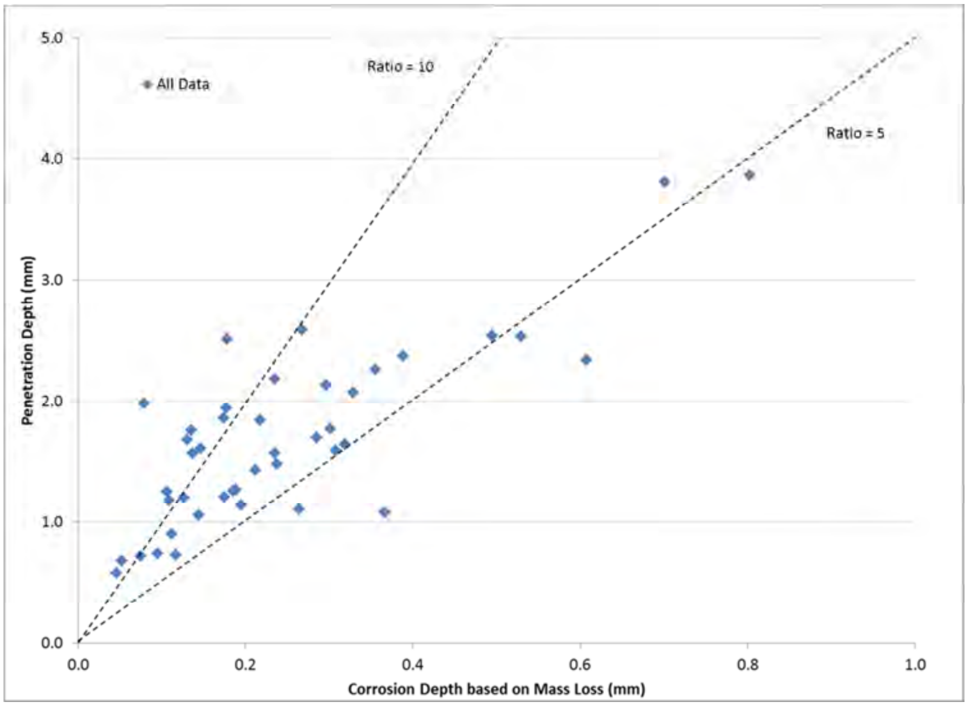

Figure 17. Plot of penetration depth as a function of corrosion depth based on mass loss, for the NBS corrosion data. All data from ~12-year retrieval time.

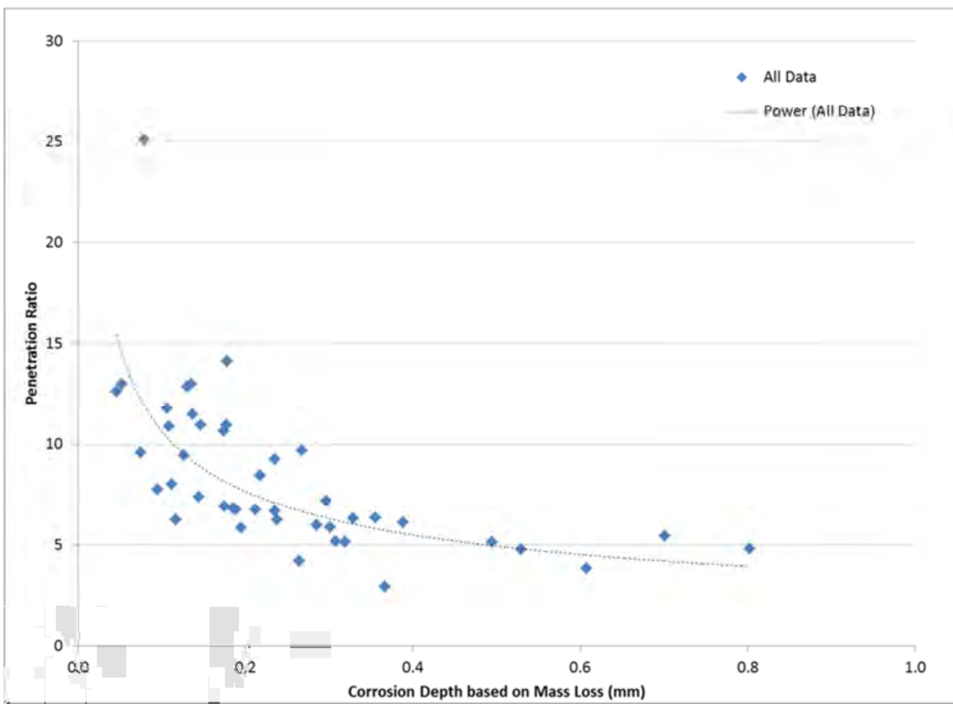

Figure 18. Plot of penetration-to-mass-loss ratio for the NBS corrosion data. All data from ~12-year retrieval time.

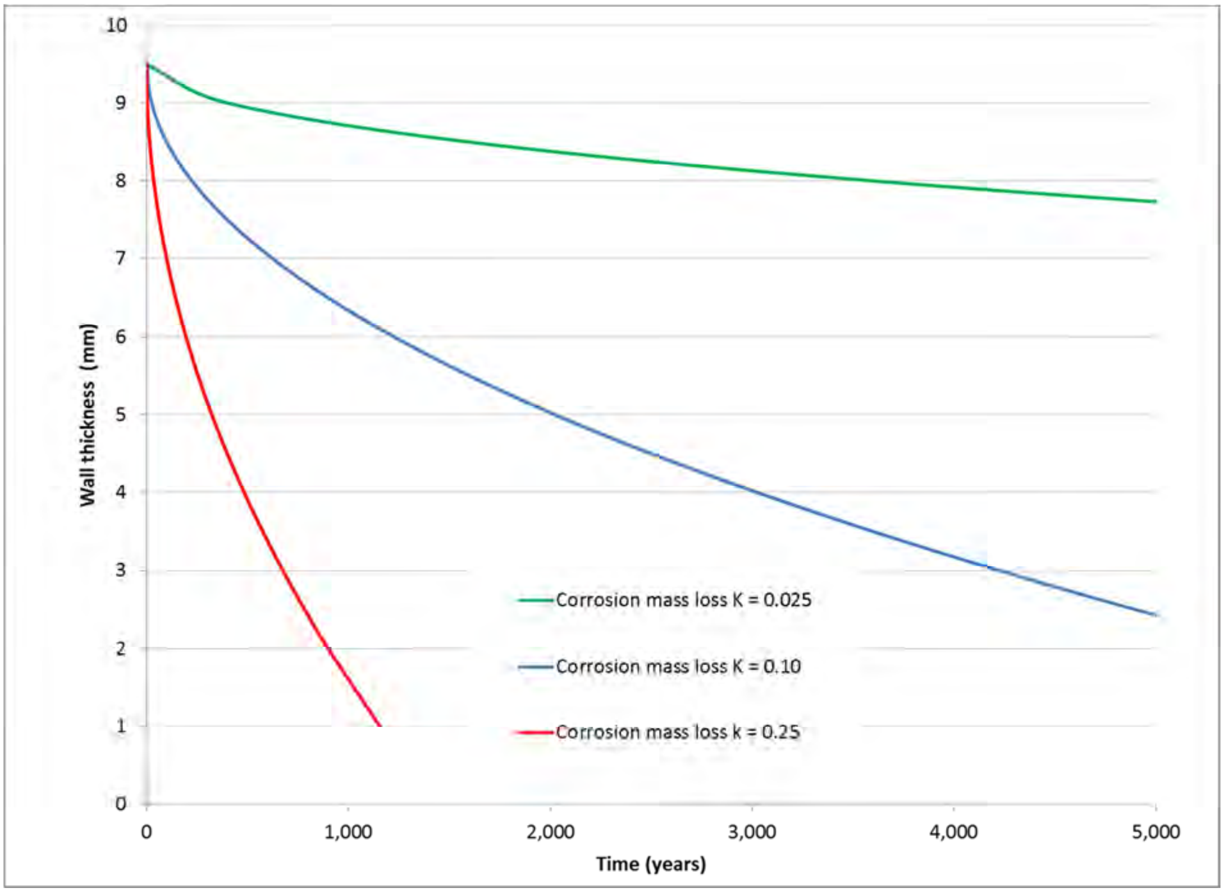

Figure 19. Plot of wall thickness as a function of time, demonstrating the effect of varying (mass loss) corrosion rates.

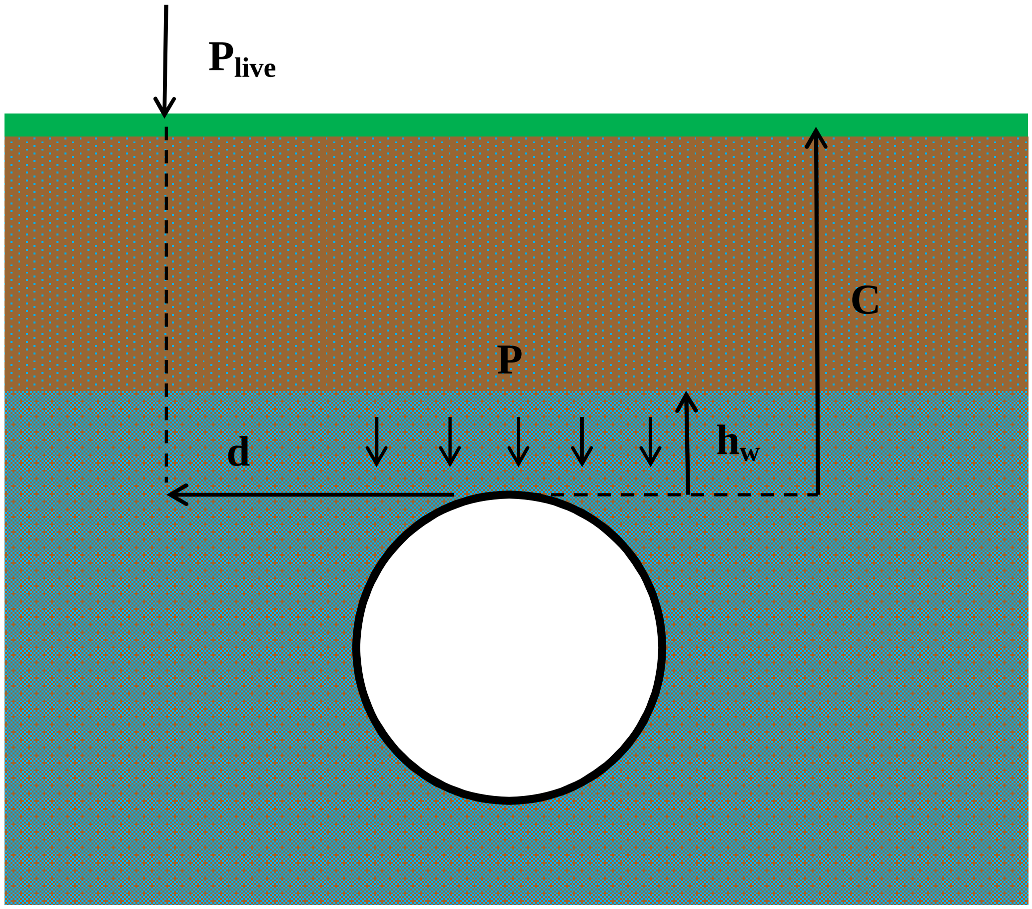

Figure 20. Schematic of the parameters used for the basic soil forces model (C is depth of cover, d is distance, h_w is water table height, P is pressure).

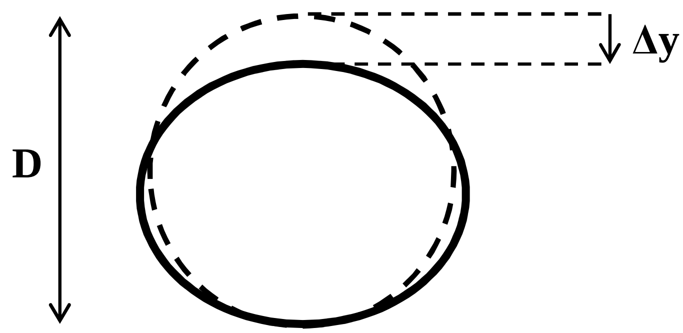

Figure 21. Illustration of the ovalization for the plastic collapse model (D is diameter, Δy is vertical deflection).

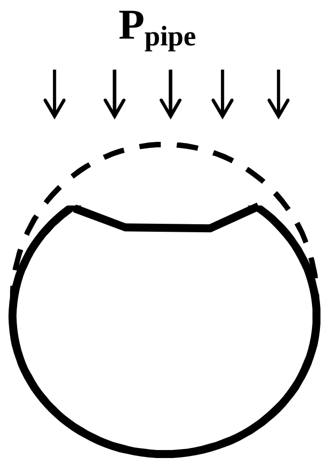

Figure 22. Illustration of buckling for the elastic collapse model.

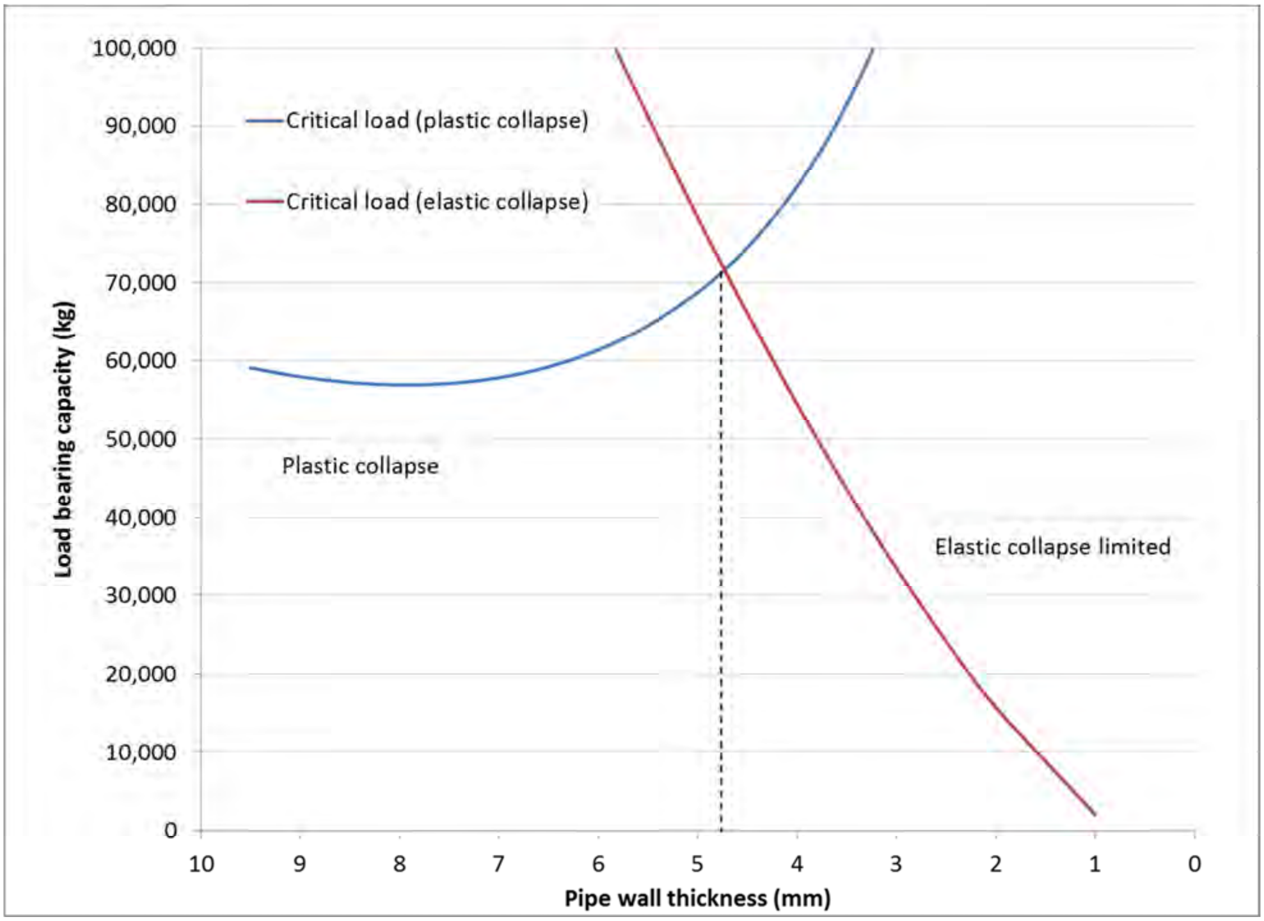

Figure 23. Plot of load bearing capacity as a function of pipe wall thickness, using the "base case" conditions.

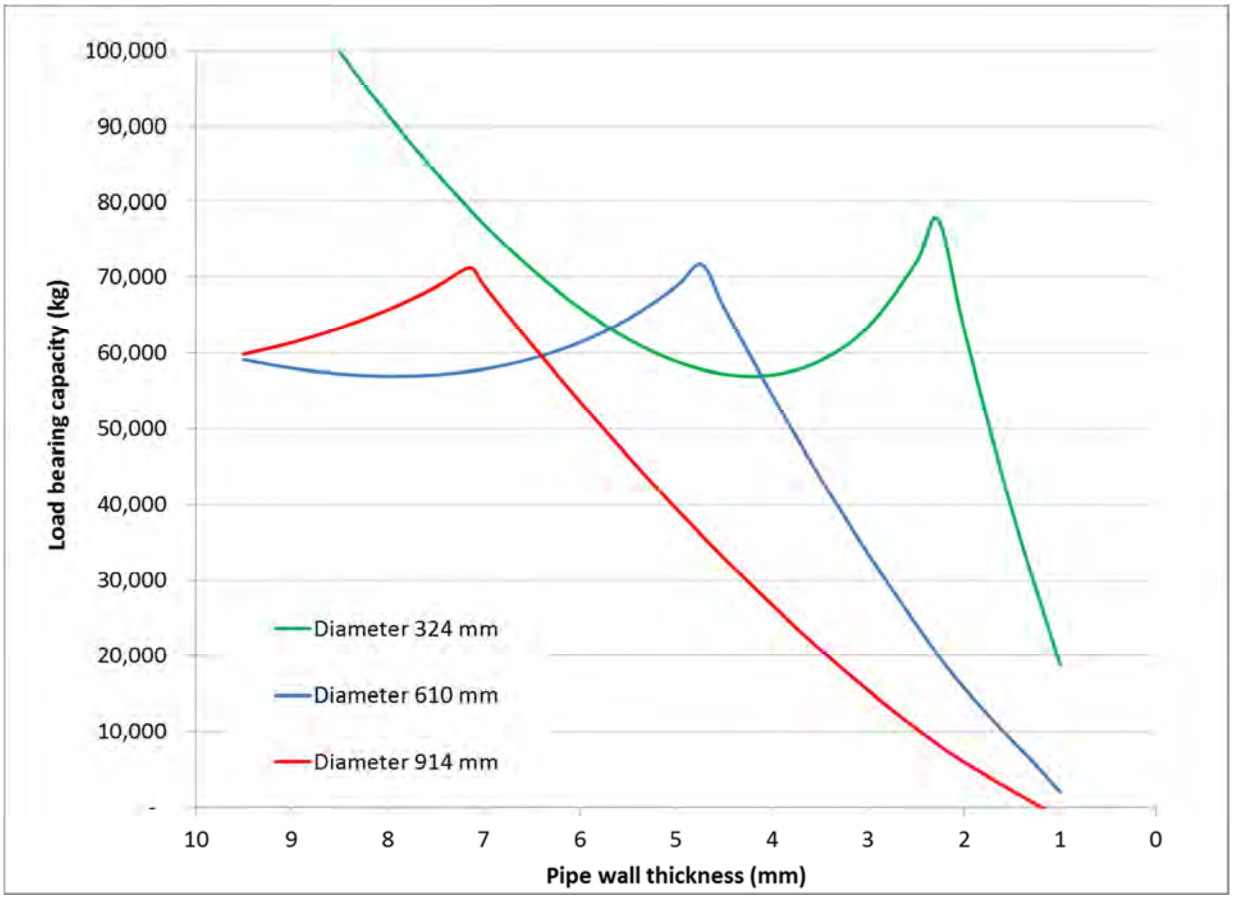

Figure 24. Plot of load bearing capacity as a function of pipe wall thickness, demonstrating the effect of varying diameter.

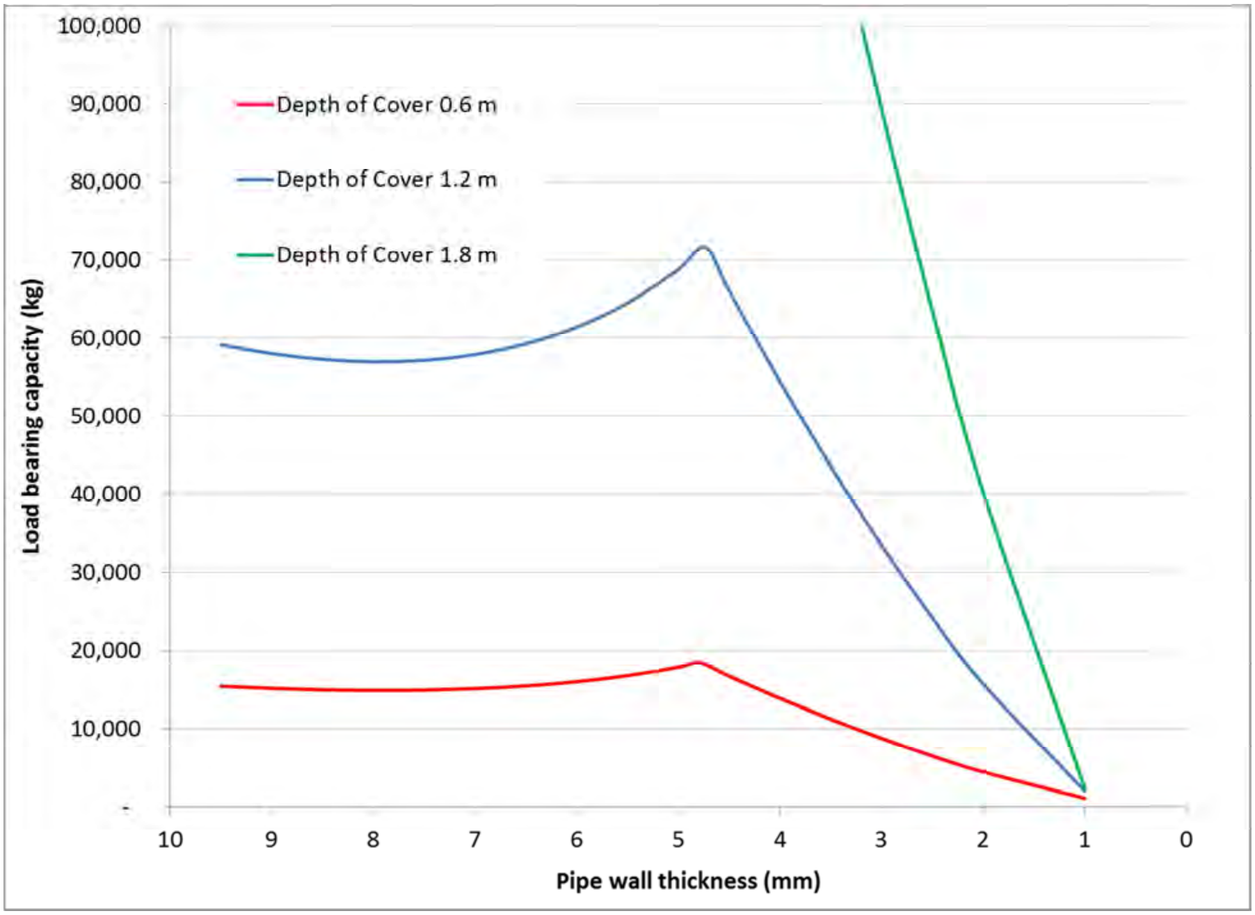

Figure 25. Plot of load bearing capacity as a function of pipe wall thickness, demonstrating the effect of varying depth of cover.

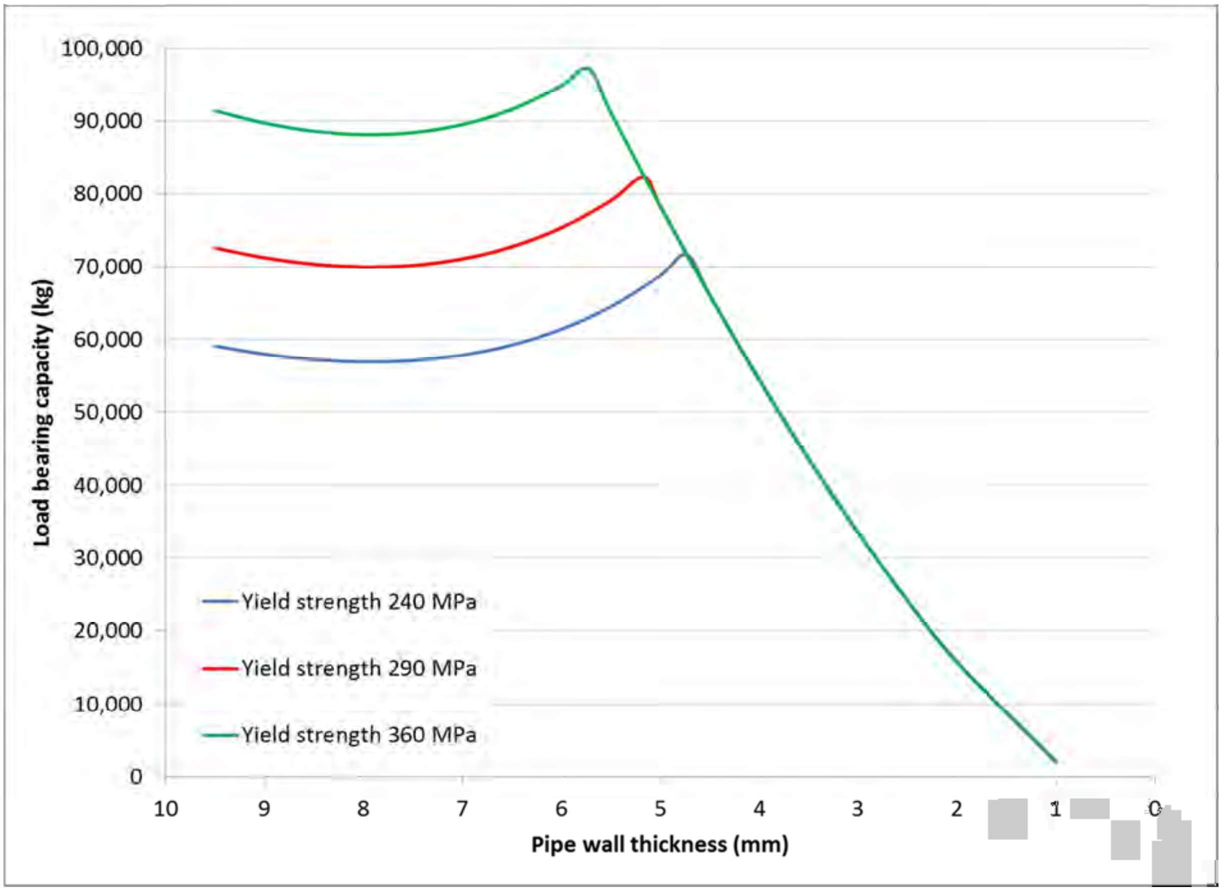

Figure 26. Plot of load bearing capacity as a function of pipe wall thickness, demonstrating the effect of varying yield strength.

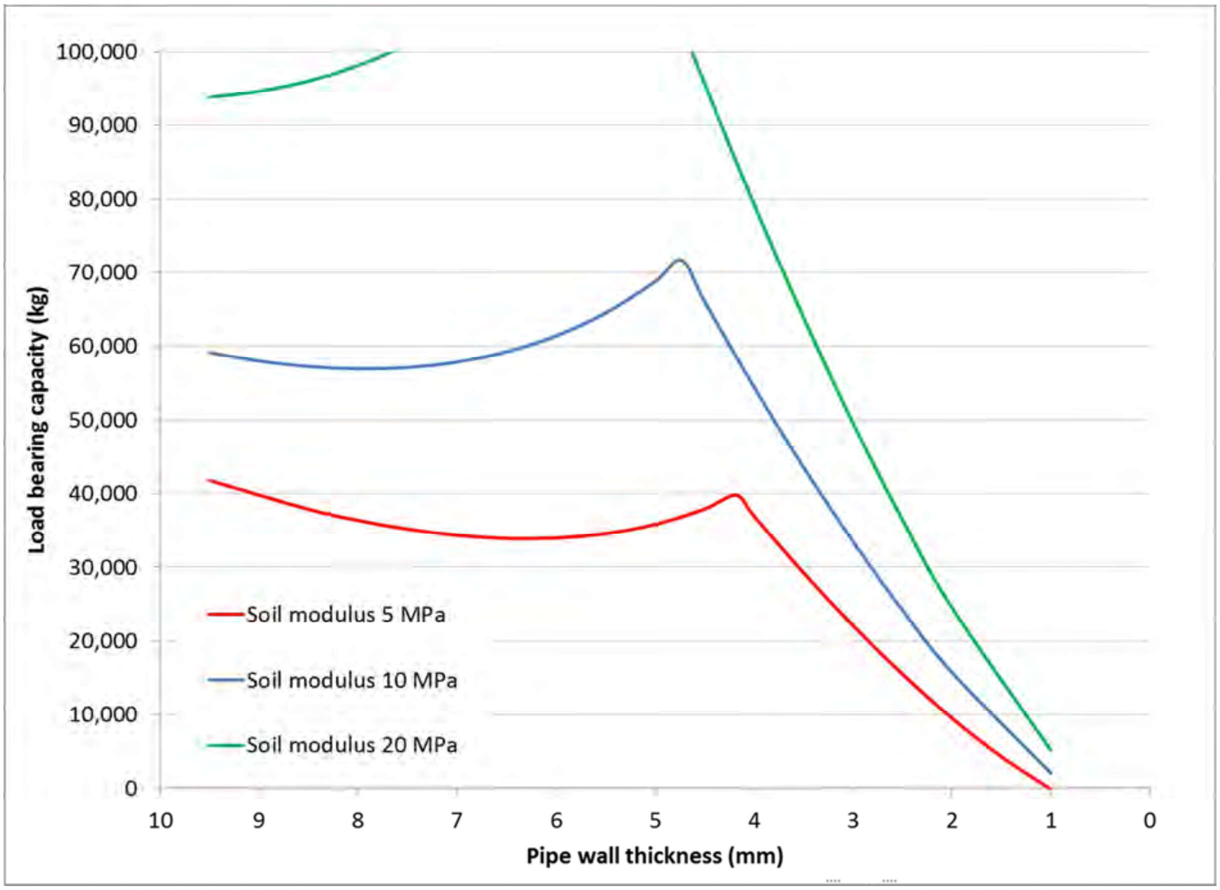

Figure 27. Plot of load bearing capacity as a function of pipe wall thickness, demonstrating the effect of varying soil modulus.

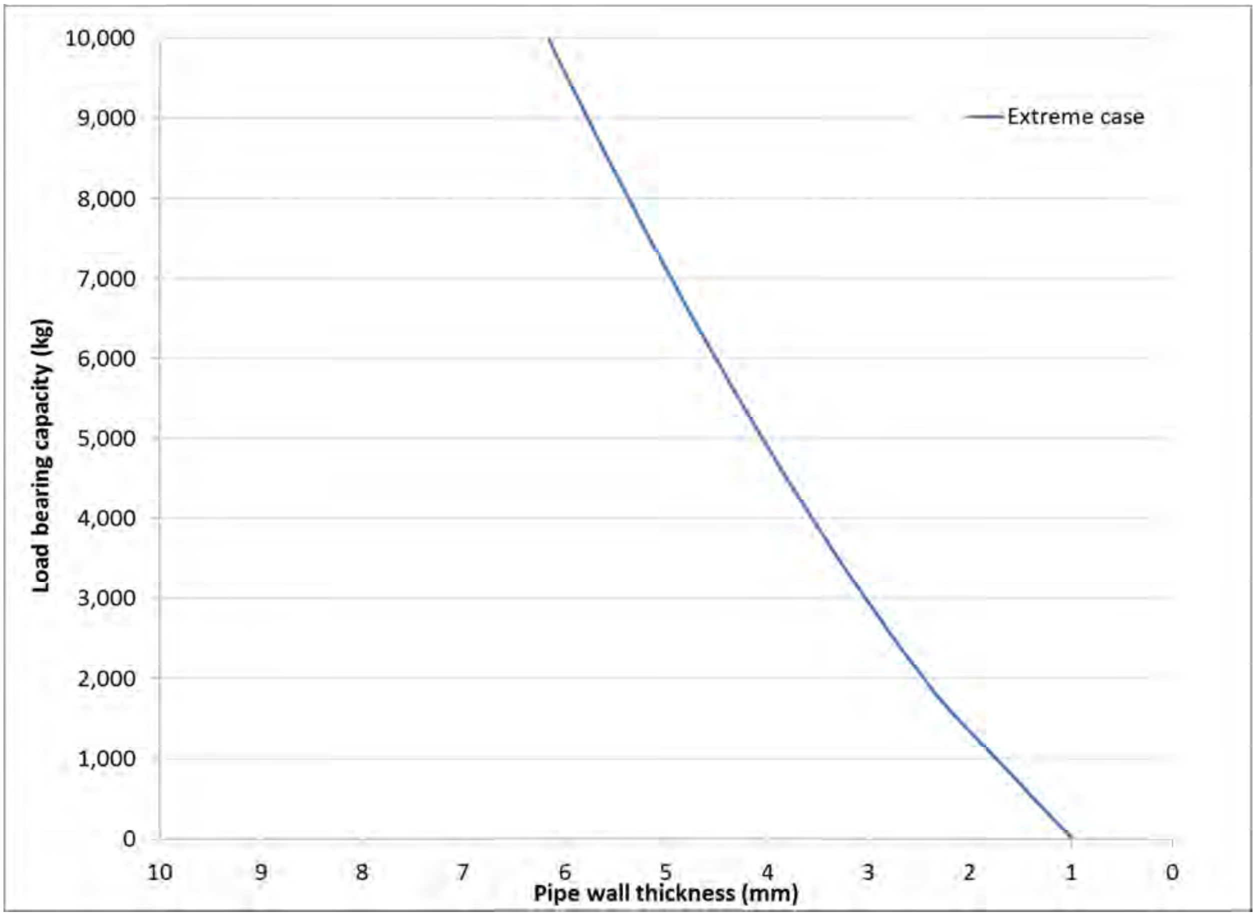

Figure 28. Plot of load bearing capacity as a function of pipe wall thickness, using "extreme case" conditions.

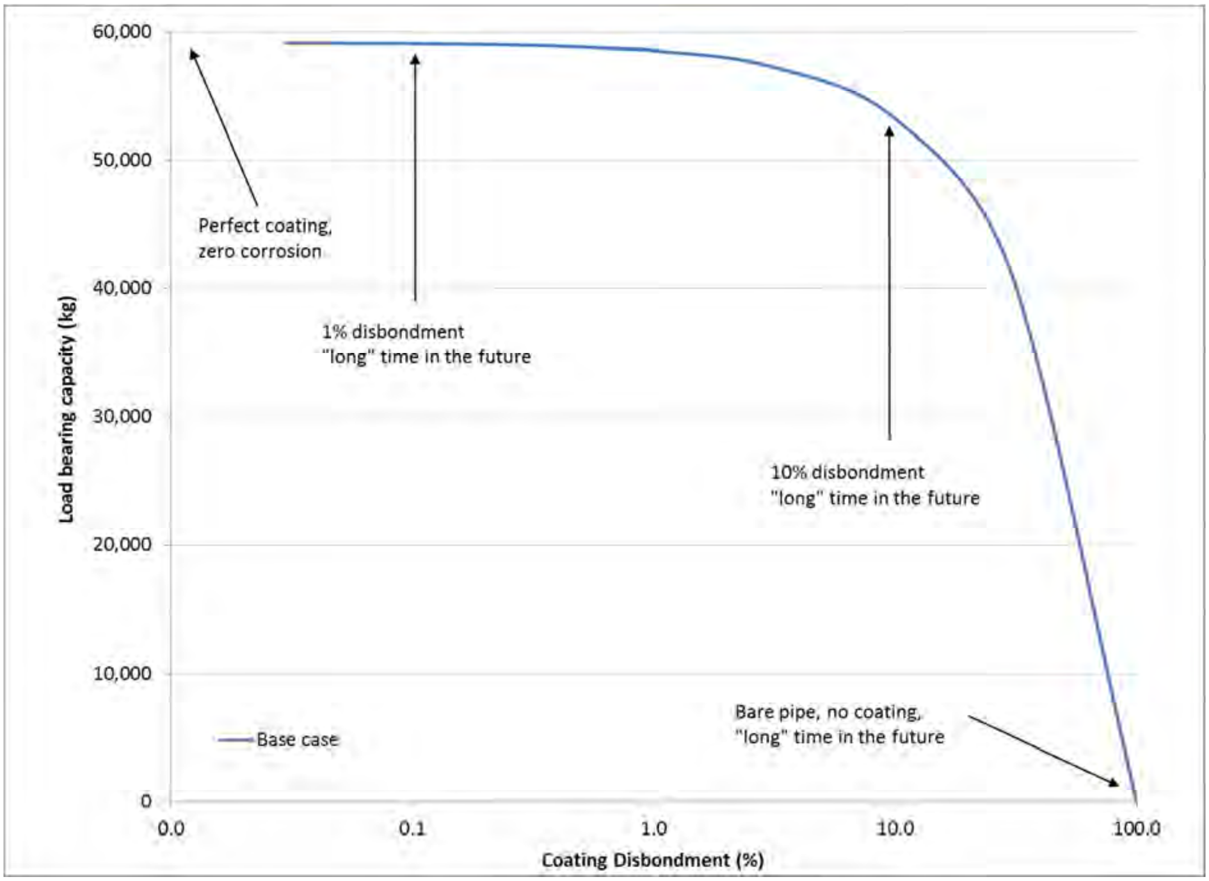

Figure 29. Plot of load bearing capacity as a function of coating disbondment, for the "base case" conditions.

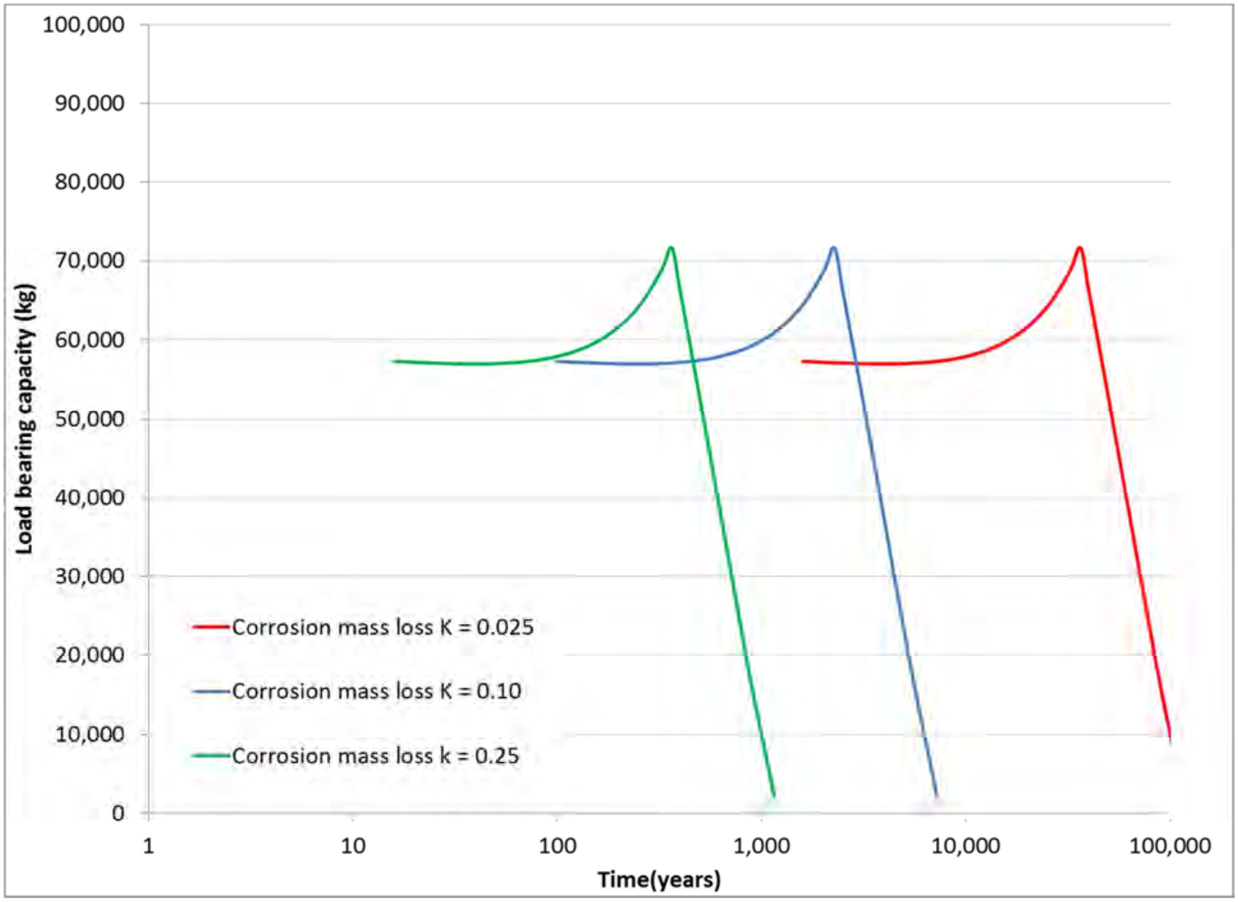

Figure 30. Plot of load bearing capacity as a function of time for the base case conditions, demonstrating the effect of varying corrosion rates.

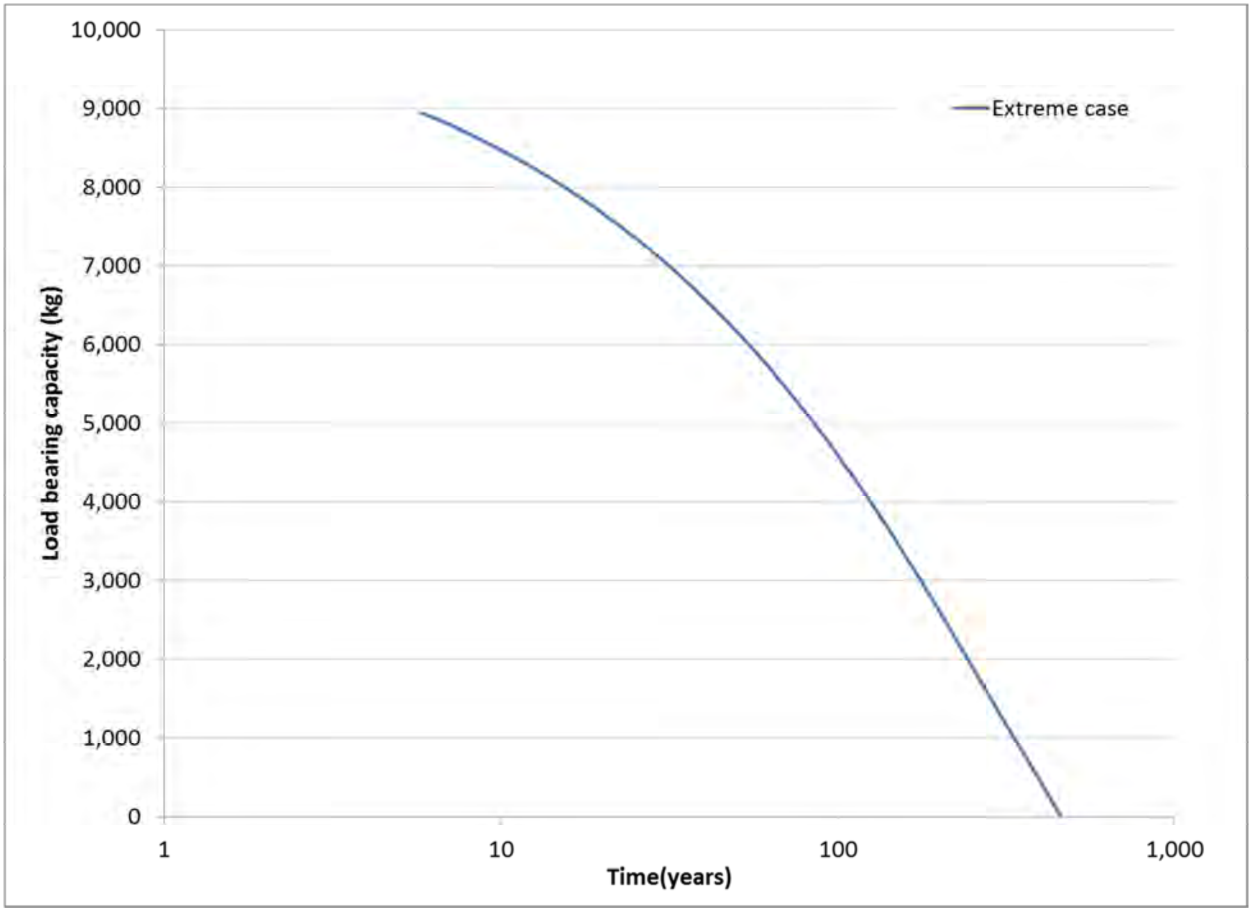

Figure 31. Plot of load bearing capacity as a function of time for the extreme case conditions, and assuming an upper bound corrosion rate from Soil #23.

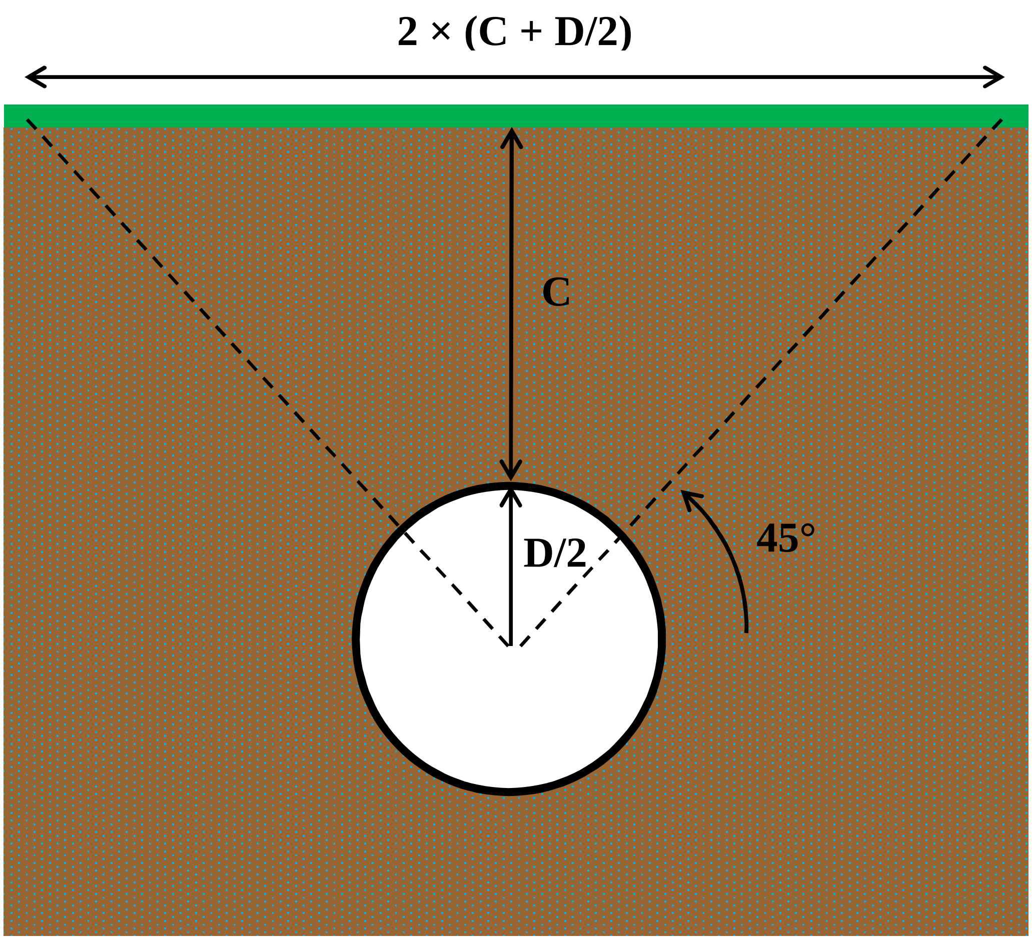

Figure 32. Schematic of geometry and soil conditions prior to pipeline collapse.

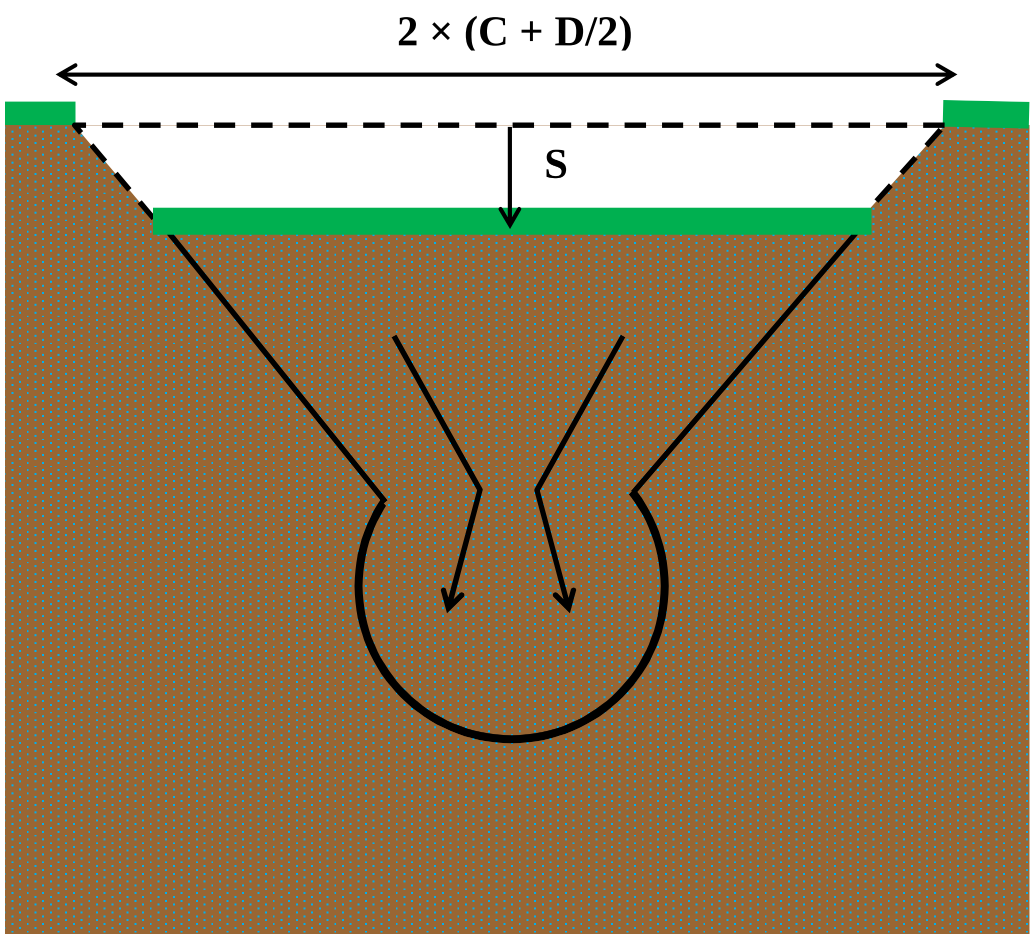

Figure 33. Schematic of geometry and soil conditions after pipeline collapse.

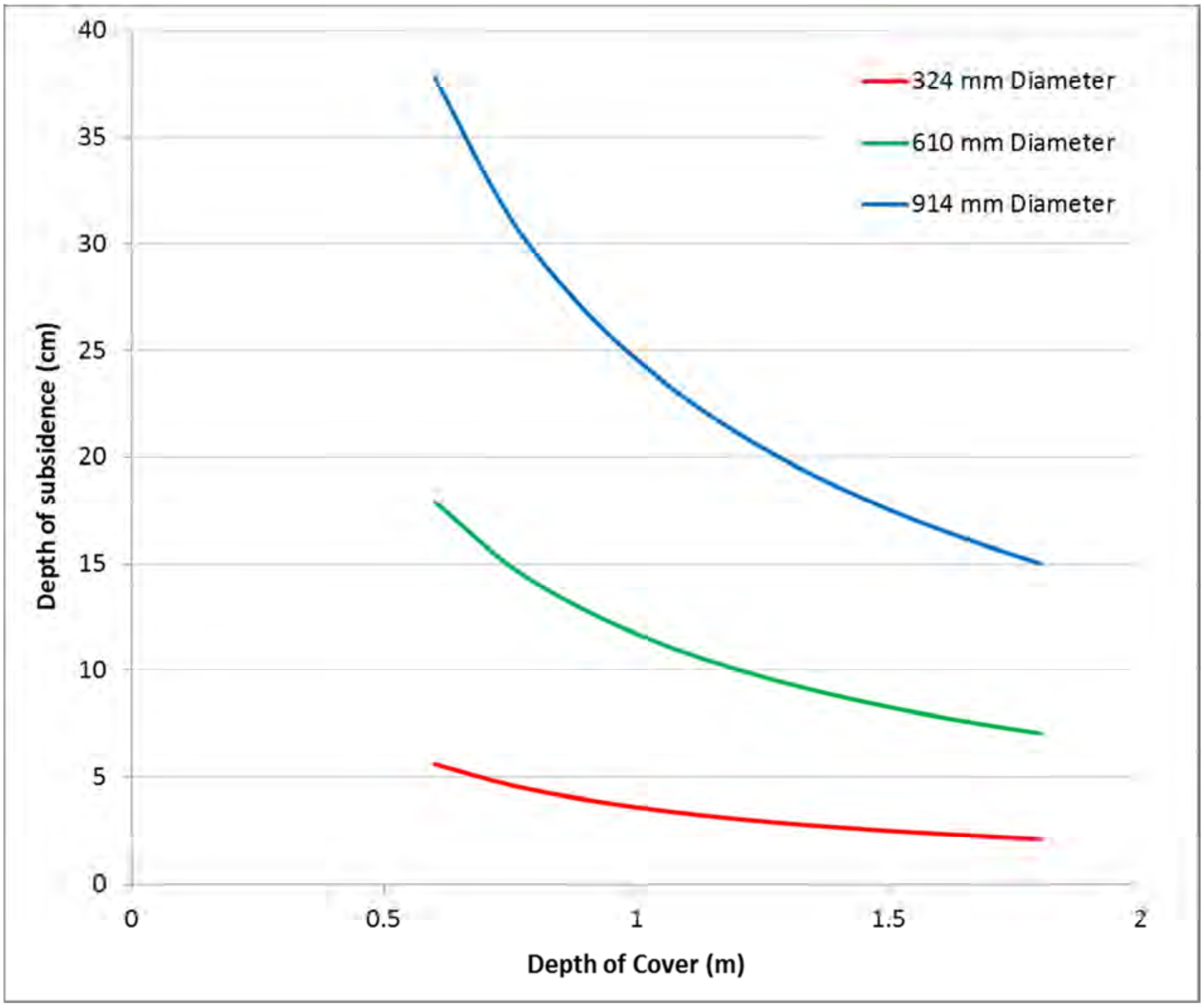

Figure 34. Plot of predicted soil subsidence depth as a function of depth of cover and pipeline diameter.

Det Norske Veritas

DNV is a global provider of knowledge for managing risk. Today, safe and responsible business conduct is both a license to operate and a competitive advantage. Our core competence is to identify, assess, and advise on risk management, and so turn risks into rewards for our customers. From our leading position in certification, classification, verification, and training, we develop and apply standards and best practices. This helps our customers to safely and responsibly improve their business performance.

Our technology expertise, industry knowledge, and risk management approach, has been used to successfully manage numerous high-profile projects around the world.

DNV is an independent organization with dedicated risk professionals in more than 100 countries. Our purpose is to safeguard life, property, and the environment. DNV serves a range of industries, with a special focus on the maritime and energy sectors. Since 1864, DNV has balanced the needs of business and society based on our independence and integrity. Today, we have a global presence with a network of 300 offices in 100 countries, with headquarters in Oslo, Norway.

Global Impact for a Safe and Sustainable Future

Learn more on www.dnv.com